

Positive geometry in the diagonal limit of the conformal bootstrap

Kallol Sen^{a*}, Aninda Sinha^{b†} and Ahmadullah Zahed^{b‡}

^a*Kavli Institute for the Physics and Mathematics of the Universe (WPI),
University of Tokyo, Kashiwa, Chiba 277-8583, Japan*

^b*Centre for High Energy Physics, Indian Institute of Science,
C.V. Raman Avenue, Bangalore 560012, India.*

Abstract

We consider the diagonal limit of the conformal bootstrap in arbitrary dimensions and investigate the question if physical theories are given in terms of cyclic polytopes. Recently, it has been pointed out that in $d = 1$, the geometric understanding of the bootstrap equations for unitary theories leads to cyclic polytopes for which the faces can all be written down and, in principle, the intersection between the unitarity polytope and the crossing plane can be systematically explored. We find that in higher dimensions, the natural structure that emerges, due to the inclusion of spin, is the weighted Minkowski sum of cyclic polytopes. While it can be explicitly shown that for physical theories, the weighted Minkowski sum of cyclic polytopes is not a cyclic polytope, it also turns out that in the large conformal dimension limit it is indeed a cyclic polytope. We write down several analytic formulae in this limit and show that remarkably, in many cases, this works out to be very good approximation even for $O(1)$ conformal dimensions. Furthermore, we initiate a comparison between usual numerics obtained using linear programming and what arises from positive geometry considerations.

Contents

1	Introduction	2
2	Diagonal limit of conformal blocks	5
2.1	Exact blocks	5
2.2	Asymptotic blocks	6

*kallolmax@gmail.com
†asinha@iisc.ac.in
‡ahmadullah@iisc.ac.in

3	Polytopes: Unitary CFT and crossing equation	7
3.1	Usual approach of CFT	7
3.2	Positive geometric approach of CFT	9
3.2.1	Positivity of the blocks	11
3.3	The crossing equation	12
4	Positivity criterion for $U[\Delta_i]$	13
4.1	Scalar blocks	13
4.2	$\Delta \gg \frac{d-2}{2}, \ell$ limit analytic results	13
4.3	Spin blocks	15
4.4	Weighted Minkowski sum	15
5	$N = 1$: Bounds on leading operator	16
5.1	Projection through identity	17
5.2	Δ_+ and Δ_- for large Δ_ϕ	18
5.3	Interpretation of Δ_+ and Δ_- from numerical bootstrap	19
6	$N = 2$: Constraints on the first two primary operators	20
7	Kink from positive geometry	22
8	Discussion	24
A	Derivation of $g_i \approx 2\sqrt{2}$ in $\Delta \gg \frac{d-2}{2}, \ell$ limit, general case.	25
B	Some examples using known theories	26
B.1	2d Ising model	26
B.2	3d Ising model	26
B.3	Different ordering of combinations of Δ and ℓ	26
C	Analytic kink analysis	28
D	Adding spin and kink	29
E	Issues with scalars	29

1 Introduction

In a CFT, the four point function of identical scalars with dimension Δ_ϕ can be written as sum over conformal blocks of exchange operator $\mathcal{O}_{\Delta,\ell}$ of scaling dimension Δ , spin ℓ with OPE coefficient (squared) $C_{\Delta,\ell}$:

$$\langle \phi(x_1) \phi(x_2) \phi(x_3) \phi(x_4) \rangle = \frac{1}{|x_{12}|^{2\Delta_\phi} |x_{34}|^{2\Delta_\phi}} \mathcal{A}(u, v) \tag{1.1}$$

with

$$\mathcal{A}(u, v) = \sum_{\Delta,\ell} C_{\Delta,\ell} G_{d,\Delta,\ell}(u, v), \tag{1.2}$$

and $C_{\Delta,\ell} > 0$ for unitary theories. Crossing symmetry implies

$$\mathcal{A}(u, v) = \left(\frac{u}{v}\right)^{\Delta_\phi} \mathcal{A}(v, u). \tag{1.3}$$

This is the usual starting point for modern studies of the conformal bootstrap. One can consider the diagonal limit of this equation which is obtained by setting $u = z\bar{z}, v = (1 - z)(1 - \bar{z})$ and taking the limit $z \rightarrow \bar{z}$. Thereby we obtain a problem in 1-variable. Following the numerical approach based on linear programming, pioneered in [1–3] and recently reviewed in [4], one can study this equation in any dimensions. Somewhat surprisingly¹, for $d = 2$, retaining only scalar operators one finds a “kink” in the plot of the allowed leading scalar operator dimension when plotted against Δ_ϕ . In figure 1, we give a comparison between the numerics obtained in the diagonal limit and what is obtained in the full problem². The kink in the diagonal problem is at $\Delta_\phi \approx 0.09, \Delta_2 \approx 1.2$ and adding other operators with spin does not appear to change the location drastically (although we have not attempted to make a thorough comparison). The full problem [5] in which there are off-diagonal derivatives, needs the inclusion of higher spin blocks before a kink appears. Furthermore, compared to the full problem where the kink appears at $\Delta_\phi \approx 0.125, \Delta_2 \approx 1$, the kink in the diagonal limit is displaced. Nonetheless, one can ask what causes the kink in this instance. In the full problem as reviewed in [4], the kink arises due to decoupling of certain operators (which happens for physical theories like the 2d Ising model due to null state conditions).

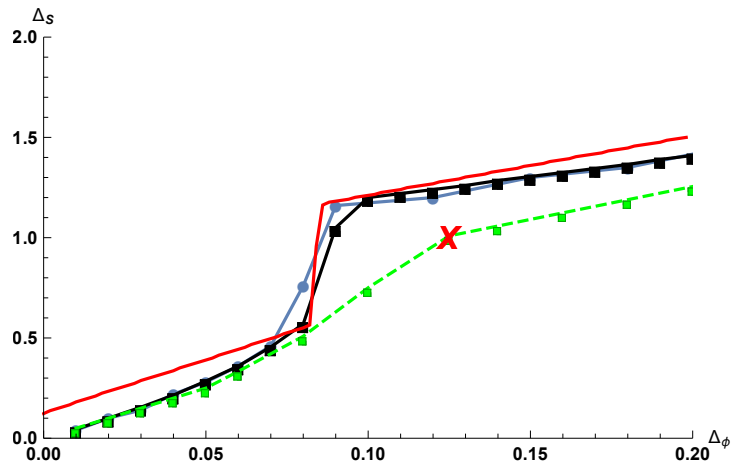


Figure 1: Plot of bounds on dimension of leading scalar in the OPE of $\phi \times \phi$ for $d = 2$ using linear programming, keeping only scalars in the spectrum in the diagonal limit. The blue line is for 10 derivatives in the functional while the black is for 20 derivatives. In each case truncating the spectrum does not change the plot much. The green line is obtained in the non-diagonal limit [5], including spins, while the red cross is the location of the 2d Ising model. The red line indicates what arises from considering the intersection of the $N = 2$ cyclic polytope obtained using scalars in $d = 2$ and the crossing plane.

Thus the diagonal limit (being somewhat simpler since it is a one variable problem) appears to be a good playground to investigate various features of the conformal bootstrap. Recently the one variable

¹This feature appears to have gone unnoticed in the literature. One can do the analogous exercise in other dimensions. For $d = 1$, there is a kink at $\Delta_\phi = 0$ which is within the unitarity limit but for $d = 3$ it is at $\Delta_\phi \sim 0.26$ and for $d = 4$ it is at $\Delta_\phi \sim 0.5$ both of which are below the unitarity bound.

²We thank Slava Rychkov for generously sharing the notebook for the full problem solved in [5]. In the approach of [1], one writes $z = 1/2 + a + b, \bar{z} = 1/2 + a - b$. If one suppresses the b derivatives in the basis, then one will recover the diagonal limit numerics in fig. 1.

bootstrap in $d = 1$ has been studied and a deep connection with the alternative approach to the bootstrap advocated in [6–12] and based on crossing symmetric Witten diagram basis expansion [8, 12], has been found [13]. Another development that has happened last year is an attempt to connect the usual conformal bootstrap program to the positive geometry of cyclic polytopes [14]. In this paper, we will endeavour to further this connection.

The work of [1] already made use of the polytope structure underlying the bootstrap equations. The idea was to rewrite the bootstrap equations in the form

$$\sum_{\Delta, \ell} C_{\Delta, \ell} \mathcal{F}_{d, \Delta, \ell}(z, \bar{z}) = 1, \quad (1.4)$$

where $\mathcal{F}_{d, \Delta, \ell}$'s are certain linear combinations of the direct and crossed-channel blocks given by

$$\mathcal{F}_{d, \Delta, \ell}(z, \bar{z}) = \frac{v^{\Delta_\phi} G_{d, \Delta, \ell}(z, \bar{z}) - u^{\Delta_\phi} G_{d, \Delta, \ell}(1 - \bar{z}, 1 - z)}{u^{\Delta_\phi} - v^{\Delta_\phi}}, \quad (1.5)$$

where $u = z\bar{z}$ and $v = (1 - z)(1 - \bar{z})$. Then, taking derivatives of the above equation around $z, \bar{z} = \frac{1}{2}$, one assumes a certain spectrum where the lowest scalar has dimension Δ_S and asks if the crossing condition can be satisfied. Using linear programming, one can rule out potential spectra and obtain bounds on Δ_S amongst other quantities. The starting point in [14] is somewhat different. One first expands the correlator (in [14] it was done in $d = 1$), in terms of the direct channel blocks. The key novel insight provided in [14] is that if Δ is not too small, then this expansion has the structure of a cyclic polytope. The reason why this is important is that the face structure of the cyclic polytope has been fully classified. This enables one to study the intersection of the crossing plane with the polytope systematically and obtain various non-trivial insights about a potential CFT satisfying the bootstrap constraints.

In this paper we will extend the work of [14] in several directions. We will consider the diagonal limit of the bootstrap equations in arbitrary dimensions. Rather than an expansion in terms of $SL(2, \mathbb{R})$ blocks, this entails an expansion in terms of the so-called diagonal blocks worked out in [15]. We will show that one can work out a systematic $1/\Delta$ expansion of the blocks³ which enables an analytic study of the results of [14]. Furthermore, the cyclic polytope picture in [14] enables us to initiate a comparison of how the kink in fig.1 is obtained in the approach of [1] and from the cyclic polytope perspective. Compared to the $d = 1$ study in [14] where the sum over spectrum only involved the conformal dimension, here we will also have to sum over spin. This creates an interesting difficulty. While for each spin, there is a cyclic polytope structure, when we sum over spins we get what is called a weighted Minkowski sum of cyclic polytopes [17]. The resulting polytope is not necessarily a cyclic polytope and one can easily check that for known CFTs like the 2d/3d Ising models, it is not. For low number of vertices, one can of course grind out the face structure. But that would miss the point made in [14]. What we find however, is that in the large Δ limit the weighted Minkowski sum is again a cyclic polytope! This means that at least in this limit, we can begin understanding (even analytically) the bootstrap problem using the positive geometry of cyclic polytopes as in [14].

³The efficacy of the $1/\Delta$ expansion has also been recently discussed in [16].

This paper is organized as follows. In section 2, we review known results about the diagonal limit of conformal blocks in arbitrary dimensions and present formulae for the leading order large Δ limit of the blocks. In section 3, we review salient features of polytopes, cyclic polytopes and conditions for the intersection of the crossing plane with the polytope. In section 4, we investigate the positivity criteria for cyclic polytopes both numerically and analytically. In sections 5 and 6 we consider the $N = 1$ and $N = 2$ polytopes and present asymptotic formulae for the bounds in [14] as well as analogous results in higher dimensions. In section 7 we initiate a study of numerical bootstrap using the cyclic polytope picture but closer in spirit to the approach [1] which used linear programming. We conclude in section 8. Some appendices support various calculations in the main text.

We will reserve the notation d for spacetime dimensions and D for the dimensionality of the polytope.

2 Diagonal limit of conformal blocks

In order to use the technology presented in [14] in higher dimensions, one would like to consider the diagonal limit of higher dimensional conformal blocks. This was worked out in [15].

2.1 Exact blocks

Unlike $d = 1$, where there are no spins, the higher dimensions the spectrum of operators are labelled by two quantum numbers: Δ and ℓ and hence a sum over these two quantum numbers⁴,

$$G_{d,\Delta,\ell}(z) = \frac{\left(\frac{z^2}{1-z}\right)^{\Delta/2} (d-2)_\ell \left(\frac{\Delta+1}{2}\right)_{\frac{\ell}{2}}}{\left(\frac{d-2}{2}\right)_\ell \left(\frac{\Delta}{2}\right)_{\frac{\ell}{2}} \left(\frac{1}{2}(-d-\ell+\Delta+3)\right)_{\frac{\ell}{2}}} \sum_{r=0}^{\frac{\ell}{2}} \frac{\left(\frac{1}{2}\right)_r \left(\frac{\ell}{2}\right)_r \left(\frac{d-2+\ell}{2}\right)_r \left(\frac{2-d+\Delta-\ell}{2}\right)_{\frac{\ell}{2}-r}}{\left(\frac{1+\Delta}{2}\right)_r} \quad (2.1)$$

$$\times {}_3F_2\left(-\frac{d}{2} + \frac{\Delta}{2} + 1, r + \frac{\Delta}{2}, \frac{\Delta}{2}; r + \frac{\Delta}{2} + \frac{1}{2}, -\frac{d}{2} + \Delta + 1; \frac{z^2}{4(z-1)}\right).$$

The ${}_3F_2$ above can again be of course again decomposed in terms of a sum over the $SL(2, R)$ blocks. We will not however venture in that direction. We note specifically, for the scalar operators,

$$G_{d,\Delta,0}(z) = \left(\frac{z^2}{1-z}\right)^{\frac{\Delta}{2}} {}_3F_2\left[1 + \frac{\Delta-d}{2}, \frac{\Delta}{2}, \frac{\Delta}{2}; \frac{\Delta+1}{2}, \Delta + 1 - \frac{d}{2}; \frac{z^2}{4(z-1)}\right]. \quad (2.2)$$

We plot the second derivative of $\mathcal{F}_{d,\Delta,\ell}$ as a function of z in fig.2 for $d = 2$. For $\Delta_\phi \lesssim 0.35$, for non-zero spin, unitary operators, the second derivative is positive around $z = 1/2$. For $\ell = 0$, the second derivative is positive for $\Delta > \Delta_S$ for some Δ_S which necessitates there being at least one scalar operator of $\Delta \leq \Delta_S$ for the bootstrap conditions to be satisfied [1]. What happens beyond $\Delta_\phi \gtrsim 0.35$ is that some non-zero spin unitary operators (beginning with $\ell = 2$) have negative second derivatives. Therefore, it is in principle possible to satisfy the bootstrap constraints in this case where we include

⁴We consider the block for the even spin. For odd spin, which will be relevant for say $O(N)$ model, the expression is slightly different [15].

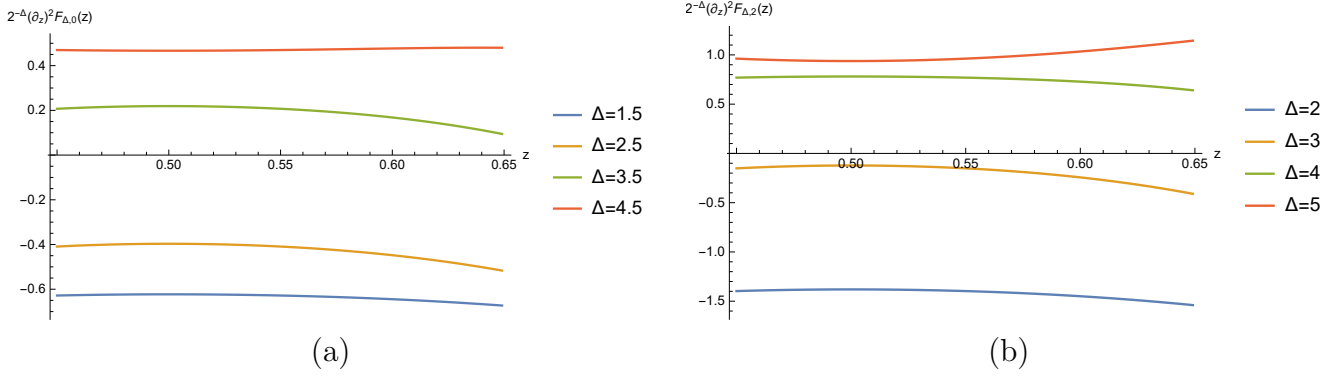


Figure 2: Plot of $\partial_z^2 \mathcal{F}_{d,\Delta,\ell}(z)$ as a function of z for $\Delta_\phi = 0.75$ in $d = 2$. For $\ell \geq 4$ for unitary $\Delta \geq \ell$, the second derivative is positive in the region shown above.

at least one operator with $\Delta_{\ell-2} \leq \Delta_T$ for some Δ_T without necessarily having a scalar $\Delta \leq \Delta_S$.

2.2 Asymptotic blocks

In this paper, at various stages we will use the large- Δ limit of the diagonal conformal blocks. The result we will need was worked out by G. N. Watson in 1914 and can be found in [18]:

$$\begin{aligned}
& {}_3F_2 \left(-\frac{d}{2} + \frac{\Delta}{2} + 1, r + \frac{\Delta}{2}, \frac{\Delta}{2}; r + \frac{\Delta}{2} + \frac{1}{2}, -\frac{d}{2} + \Delta + 1; Z \right) \sim \\
& \frac{\left(\frac{1-\sqrt{1-Z}}{Z} \right)^{-\frac{d}{2}} \left(2^{\Delta-\frac{d}{2}} (-Z + 2\sqrt{1-Z} + 2)^{-\frac{\Delta}{2}} \right)}{\sqrt{-Z - 2\sqrt{1-Z} + 2}} \left[\left(\sqrt{1-Z} - 1 \right) - \frac{(Z + 2\sqrt{1-Z} - 2)(d^2 - 6d - 8r + 4)}{8\Delta} \right. \\
& \left. + O\left(\frac{1}{\Delta^2}\right) \right]
\end{aligned} \tag{2.3}$$

where $Z = \frac{z^2}{4(z-1)}$. In terms [15] of $Z = -\frac{4\rho^2}{(1-\rho^2)^2}$, or $z = \frac{4\rho}{(1+\rho)^2}$, with $0 \leq \rho \leq 1$, this is very simply

$$(1 - \rho^2)^{\Delta - \frac{d}{2}} \left[1 + \frac{(d^2 - 6d - 8r + 4)}{8\Delta} \left(\frac{2\rho^2}{1 - \rho^2} \right) + O\left(\frac{1}{\Delta^2}\right) \right].$$

Under the crossing transformation $z \rightarrow 1 - z$, $\rho \rightarrow \frac{(1-\sqrt{\rho})^2}{(1+\sqrt{\rho})^2}$. This variable naturally arises in the large Δ asymptotics [1]. The blocks are analytic in the z plane except for the cut $(1, \infty)$. ρ maps the cut plane to a unit disc and can also be thought of as lightcone coordinates in higher dimensions [19]. The general form is that the $1/\Delta^n$ term in the series inside the bracket comes with $p_n(\rho^2, r, d)/(1 - \rho^2)^n$ where $p_n(\rho^2, r, d)$ is a polynomial in ρ^2, r, d of degrees $n, n, 2n$ respectively. Many subleading orders can be systematically worked out following [18]. An interesting thing to notice is that the sub-leading term for $r = 0$ changes sign when $d > 6$. We do not know if this is of any significance.

Now using eq.(2.3) in eq.(2.1), we get

$$G_{d,\Delta,\ell}(z) \sim \frac{\sqrt{\pi} 2^{\Delta+\frac{1}{2}} (\sqrt{1-Z}+1)^{d/2} \left(\frac{Z}{Z+2\sqrt{1-Z}-2}\right)^{-\frac{\Delta}{2}} \Gamma(-\frac{d}{2}+\Delta+1) (d-2)_\ell \left(\frac{\Delta+1}{2}\right)_{\frac{\ell}{2}}}{\sqrt{\Delta} \Gamma\left(\frac{\Delta-1}{2}\right) \Gamma\left(\frac{1}{2}(-d+\Delta+3)\right) \left(\frac{d-2}{2}\right)_\ell \left(\frac{\Delta}{2}\right)_{\frac{\ell}{2}}} \sum_{r=0}^{\ell/2} \frac{\left(\frac{1}{2}\right)_r \left(\frac{\ell}{2}\right)_r \left(\frac{1}{2}(d+\ell-2)\right)_r \left(\frac{1}{2}(-d-\ell+\Delta+2)\right)_{\frac{1}{2}(\ell-2r)}}{\left(\frac{\Delta+1}{2}\right)_r \left(\frac{1}{2}(-d-\ell+\Delta+3)\right)_{\frac{\ell}{2}}} \left(1 + O\left(\frac{1}{\Delta}\right)\right) \quad (2.4)$$

where $Z = \frac{z^2}{4(z-1)}$. Then doing the r sum and using the Saalschutz formula

$${}_3F_2\left(\frac{1}{2}, \frac{d}{2} + \frac{\ell}{2} - 1, -\frac{\ell}{2}; \frac{d}{2} - \frac{\Delta}{2}, \frac{\Delta}{2} + \frac{1}{2}; 1\right) = \frac{\left(\frac{\Delta}{2}\right)_{\ell/2} \left(\frac{1}{2}(d-\Delta-1)\right)_{\ell/2}}{\left(\frac{\Delta+1}{2}\right)_{\ell/2} \left(\frac{d-\Delta}{2}\right)_{\ell/2}}, \quad (2.5)$$

we finally get to the leading order,

$$G_{d,\Delta,\ell}^{approx}(z) \sim \frac{\sqrt{\pi} 2^{-\frac{3d}{2}+2\Delta+3} (\sqrt{1-Z}+1)^{d/2} \left(\frac{Z}{Z+2\sqrt{1-Z}-2}\right)^{-\frac{\Delta}{2}} \Gamma(d+\ell-2)}{\Gamma\left(\frac{d-1}{2}\right) \Gamma\left(\frac{d}{2}+\ell-1\right)} [1 + O(\Delta^{-1})]. \quad (2.6)$$

In terms the ρ variable, we note

$$\left(\sqrt{1-Z}+1\right)^{d/2} \left(\frac{Z}{Z+2\sqrt{1-Z}-2}\right)^{-\frac{\Delta}{2}} = 2^{d/2} (1-\rho^2)^{-d/2} \rho^\Delta.$$

We plot below the ratio of exact and asymptotic blocks. From fig.(3) it is clear that eq.(2.6) is a reasonable approximation (upto 1% error for even $\Delta \sim O(1)$). In many calculations below⁵, we will make use of these asymptotic blocks and derive analytical formulae which explain several numerical results arising from using the exact blocks.

3 Polytopes: Unitary CFT and crossing equation

3.1 Usual approach of CFT

In this section, we will summarize certain key geometric ideas given in [14] as well as [1] which will be used in the paper. To start with, we consider the geometric meaning of the sum rule presented in eq. (1.4) in the diagonal limit.

$$\mathcal{F}_{d,\Delta,\ell}(z) = \frac{(1-z)^{2\Delta_\phi} G_{d,\Delta,\ell}(z) - z^{2\Delta_\phi} G_{d,\Delta,\ell}(1-z)}{z^{2\Delta_\phi} - (1-z)^{2\Delta_\phi}}, \quad (3.1)$$

In any dimension d , given a span of vectors $\mathcal{F}_{d,\Delta,\ell}(z)$ for a spectrum $\{\Delta, \ell\}$, does eq.(1.4) admit a solution with arbitrary positive definite coefficients $C_{\Delta,\ell}$?

⁵We have worked out up to $1/\Delta^3$ terms in the asymptotic expansion but refrain from showing the hideous expressions in the main text.

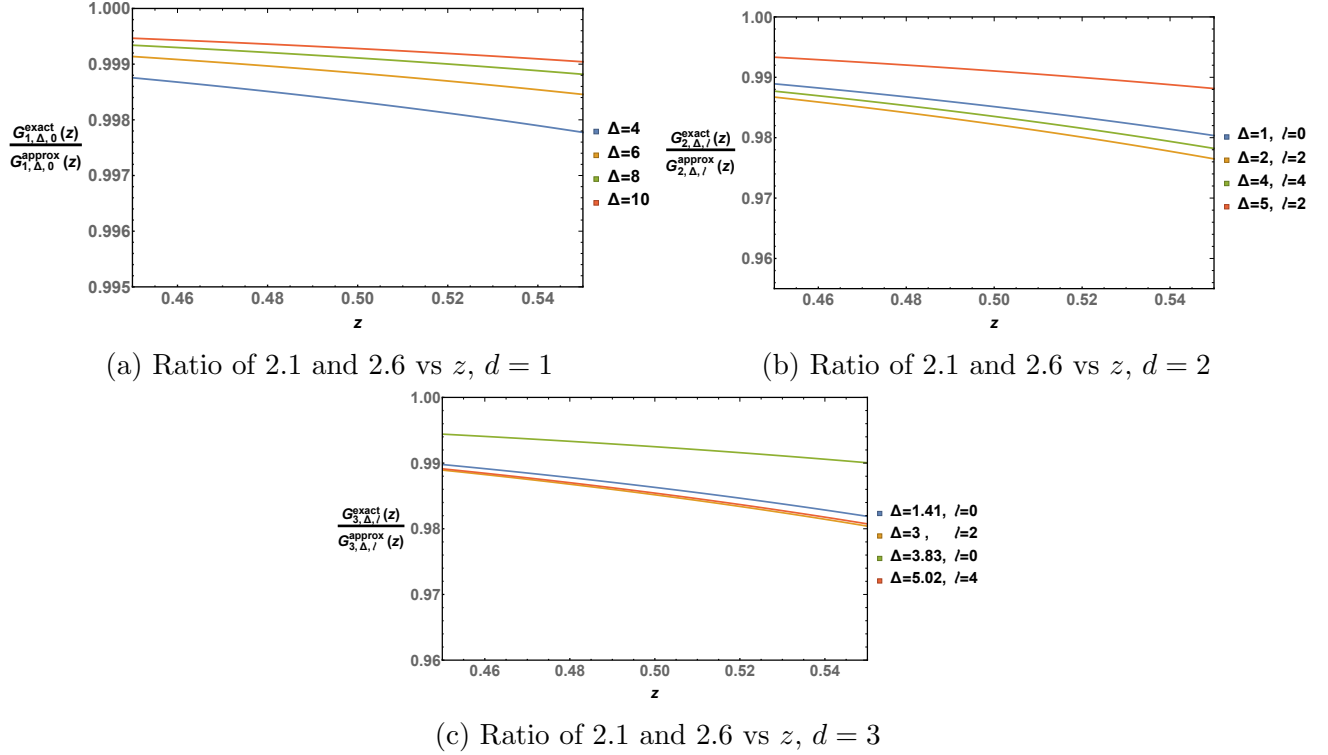


Figure 3: Ratio of 2.1 and 2.6 vs z for various Δ and ℓ . As is clear eq.(2.6) gives an excellent approximation to the exact blocks for physical values of Δ, ℓ to within a few percent.

The *rhs* of (1.4) defines a convex cone \mathcal{C} in the space of functions $\{\mathcal{F}_{d,\Delta,\ell}(z)\}$. In order to proceed it is necessary to parameterize the space of functions $\{\mathcal{F}_{d,\Delta,\ell}(z)\}$. This is achieved by replacing the functional space by a discrete infinite vector space of derivatives of $\mathcal{F}_{d,\Delta,\ell}(z)$ at some symmetric point. For convenience the most symmetric point (as also the most convergent point of expansion) is $z = 1/2$. The vector space is made of even derivatives⁶,

$$\mathcal{B} = \{\mathcal{F}_{d,\Delta,\ell}^{2m}\} = \left\{ \partial_z^{2m} \mathcal{F}_{d,\Delta,\ell}(z) \Big|_{z=1/2} \right\}. \quad (3.2)$$

while the odd derivatives vanish due to crossing symmetry in (3.1). In terms of the basis, (3.1) can be written as a set of infinite relations for $m \geq 0$,

$$\sum_{\Delta,\ell} C_{\Delta,\ell} \mathcal{F}_{d,\Delta,\ell}^{2m} = \begin{cases} 1, & m = 0 \\ 0, & m > 0 \end{cases}. \quad (3.3)$$

The key idea is to identify the linear functional,

$$\Lambda : \Lambda(\mathcal{F}_{d,\Delta,\ell}) = \sum_{\mathcal{B}} \lambda_{2m} \mathcal{F}_{d,\Delta,\ell}^{2m}, \quad (3.4)$$

⁶We have borrowed notation from [1]

such that, (1.4) can be checked via numerical methods such as *Linear Programming*. Refraining from the details which are explained nicely in [1], the essence of the approach is:

- Assume a spectrum consistent with unitarity and assuming that scalars have dimension $\Delta \geq \Delta_S$.
- A solution to the linear programming problem gives a set of λ_{2m} such that $\sum_{\Delta,\ell} C_{\Delta,\ell} \lambda_{2m} \mathcal{F}_{\Delta,\ell}^{2m} > 0$. In other words for such a spectrum it is not possible to satisfy eq.(3.3) since this is nothing but a linear combination of the equations in eq.(3.3).
- Reduce Δ_S such that no solution to the linear programming problem is found. This corresponds to a potentially allowed spectrum.

3.2 Positive geometric approach of CFT

The approach taken by [14] is somewhat different and makes use of the known faces of what is called a cyclic polytope. Instead of starting with eq.1.4, one can equivalently consider the convex cone \mathcal{C} or more specifically the *convex hull* of vectors built from the conformal blocks themselves.

Specifically, one truncates the Taylor series of the four-point function, which in turn is expanded in terms of the direct channel conformal blocks, upto some say $2N + 2$ terms around $z = 1/2$

$$\begin{aligned} \mathcal{A}(z) &= \mathcal{A}^0 + \mathcal{A}^1 y + \mathcal{A}^2 y^2 + \dots + \mathcal{A}^{2N+1} y^{2N+1} \\ G_{d,\Delta,\ell}(z) &= G_{d,\Delta,\ell}^0 + G_{d,\Delta,\ell}^1 y + G_{d,\Delta,\ell}^2 y^2 + \dots + G_{d,\Delta,\ell}^{2N+1} y^{2N+1} \end{aligned} \quad (3.5)$$

where $y \equiv z - 1/2$ and $\mathcal{A}^n = \frac{1}{n!} \partial_z^n \mathcal{A}(z) \Big|_{z=1/2}$, $G_{d,\Delta,\ell}^n = \frac{1}{n!} \partial_z^n G_{d,\Delta,\ell}(z) \Big|_{z=1/2}$. Therefore \mathcal{A} lies in the positive span of the block vector $\mathbf{G}_{d,\Delta,\ell}$

$$\mathcal{A} = \sum_{\Delta,\ell} C_{\Delta,\ell} \mathbf{G}_{d,\Delta,\ell}, \quad (3.6)$$

where $C_{\Delta,\ell} > 0$ for unitary theories and,

$$\mathcal{A}(z) \rightarrow \mathcal{A} = \begin{pmatrix} \mathcal{A}^0 \\ \mathcal{A}^1 \\ \vdots \\ \mathcal{A}^{2N+1} \end{pmatrix} \in \mathbb{P}^{2N+1} \quad \text{and} \quad G_{d,\Delta,\ell}(z) \rightarrow \mathbf{G}_{d,\Delta,\ell} = \begin{pmatrix} G_{d,\Delta,\ell}^0 \\ G_{d,\Delta,\ell}^1 \\ \vdots \\ G_{d,\Delta,\ell}^{2N+1} \end{pmatrix} \in \mathbb{P}^{2N+1}. \quad (3.7)$$

The dimensionality D of the polytope is $D = 2N + 1$. To make \mathbb{P}^{2N+1} explicit, we note that the above equation 3.6 tells us that since we can trivially multiply both sides by a non-zero number (absorbing this into the $C_{\Delta,\ell}$'s on the rhs), we can equivalently consider the expansion of $\mathcal{A} \rightarrow t \mathcal{A}$. Similarly the cone spanned by $\mathbf{G}_{d,\Delta,\ell}$ is same as $\mathbf{G}_{d,\Delta,\ell} \rightarrow \alpha_{\Delta,\ell} \mathbf{G}_{d,\Delta,\ell}$ with $\alpha_{\Delta,\ell} > 0$ since we can again absorb this into the OPE coefficients. In other words we can expand

$$\mathcal{A} = t \begin{pmatrix} 1 \\ \vec{\mathcal{A}} \end{pmatrix} \quad \text{in terms of} \quad \mathbf{G}_{d,\Delta,\ell} = \alpha_{\Delta,\ell} \begin{pmatrix} 1 \\ \vec{G}_{d,\Delta,\ell} \end{pmatrix}, \quad (3.8)$$

Now plugging back in to the equation 3.6 gives $\sum \alpha_{\Delta,\ell} C_{\Delta,\ell} \equiv \sum C'_{\Delta,\ell} = t$. Therefore we can write the equation 3.6 as

$$\vec{\mathcal{A}} = \sum_{\Delta,\ell} \lambda_{\Delta,\ell} \vec{G}_{d,\Delta,\ell}, \quad (3.9)$$

where $\lambda_{\Delta,\ell} = \frac{C'_{\Delta,\ell}}{\sum C'_{\Delta,\ell}}$. Also note that $\sum_{\Delta,\ell} \lambda_{\Delta,\ell} = 1$ which defines convex hull of $\vec{G}_{d,\Delta,\ell}$ which is a polytope in \mathbb{R}^{2N+1} . Therefore more generally we can think of the equation (3.6) as projective polytope in \mathbb{P}^{2N+1} .

It is also possible to define the polytope by a collection of hyperplanes W_{aI} , the facets, that cut out the polytope by the linear inequalities. Here \mathbf{W}_a defines a collection of hyperplanes and

$$\mathcal{A} \cdot \mathbf{W}_a = \mathcal{A}^I W_{aI} > 0, \quad (3.10)$$

outline the structure of the polytope. It is difficult to check whether a given vector lies inside or outside a polytope. This is because the representation of \mathcal{A} is non-unique. By contrast the facet definition does allow us to practically check whether or not a given \mathcal{A} is inside or not by simply checking the inequalities.

Now given a polytopes in \mathbb{P}^D , the facets for the convex hull of a set of vectors \mathbf{v}_i ⁷ are given by the set of D vectors $(\mathbf{v}_{i_1}, \mathbf{v}_{i_2}, \dots, \mathbf{v}_{i_D})$ such that [14],

$$\langle \mathbf{v}_i, \mathbf{v}_{i_1}, \mathbf{v}_{i_2}, \dots, \mathbf{v}_{i_D} \rangle \text{ have same sign ; } \forall i. \quad (3.11)$$

The corresponding facets defining the boundary of the polytope are,

$$W_{aI} = \epsilon_{II_1 \dots I_D} v_{i_1}^{I_1} \dots v_{i_D}^{I_D}. \quad (3.12)$$

There is a class of polytope which vertices have an ordering v_1, \dots, v_n where n can be larger than D , such that [14].

$$\langle \mathbf{v}_{i_1}, \mathbf{v}_{i_2}, \dots, \mathbf{v}_{i_D} \rangle, \text{ have same sign } \forall i_1 < i_2 < \dots < i_D. \quad (3.13)$$

Such structures can be analytically computed for any \mathbb{P}^D and form the *cyclic polytope*. The facets of a cyclic polytope are given by [14]

$$\begin{aligned} \text{D odd: } \{ \mathbf{W}_a \} &= \left(\mathbf{v}_1, \mathbf{v}_{i_1}, \mathbf{v}_{i_1+1}, \mathbf{v}_{i_2}, \mathbf{v}_{i_2+1}, \dots, \mathbf{v}_{i_{\frac{D-1}{2}}}, \mathbf{v}_{i_{\frac{D-1}{2}+1}} \right) \\ &\cup (-1) \left(\mathbf{v}_{i_1}, \mathbf{v}_{i_1+1}, \mathbf{v}_{i_2}, \mathbf{v}_{i_2+1}, \dots, \mathbf{v}_{i_{\frac{D}{2}-1}}, \mathbf{v}_{i_{\frac{D-1}{2}+1}}, \mathbf{v}_n \right), \\ \text{D even: } \{ \mathbf{W}_a \} &= \left(\mathbf{v}_{i_1}, \mathbf{v}_{i_1+1}, \mathbf{v}_{i_2}, \mathbf{v}_{i_2+1}, \dots, \mathbf{v}_{i_{\frac{D}{2}}}, \mathbf{v}_{i_{\frac{D}{2}+1}} \right). \end{aligned} \quad (3.14)$$

⁷ \mathbf{v}_i or simply “ i ” in determinants are short hand notation for the components of $\mathbf{G}_{d,\Delta_i,\ell_i}$

3.2.1 Positivity of the blocks

From the point of view of the CFT spectrum, the block vectors can be ordered simply in terms of increasing Δ . This would mean that the spins are not necessarily ordered. Additionally there are two more vectors $\mathbf{v}_0 = (1, 0, \dots, 0)$ and $\mathbf{v}_\infty = (0, \dots, 0, 1)$ which represent the identity operator and the $\Delta = \infty$ operator as a part of the spectrum. In order to show that block vectors $\mathbf{G}_{d,\Delta,\ell}$ form a cyclic polytope we proceed as below: First we have an ordered set of vectors $(i_1, i_2, \dots, i_{D+1})$ such that $\Delta_{i_1} < \Delta_{i_2} < \dots < \Delta_{i_{D+1}}$. Then in terms of the condition for positivity discussed in [14], the condition for a cyclic polytope is

$$\langle i_1, i_2, \dots, i_{D+1} \rangle \equiv \epsilon_{I_1 I_2 \dots I_{D+1}} G_{d,\Delta_{i_1},\ell}^{I_1} \dots G_{d,\Delta_{i_{D+1}},\ell}^{I_{D+1}} \text{ have the same sign.} \quad (3.15)$$

In order to proceed from here we define,

$$F_{m,n} = \frac{1}{m!} \partial_\Delta^n \partial_z^m G_{d,\Delta,\ell}(z)|_{z=1/2}. \quad (3.16)$$

Then we construct the \mathbf{K}_{2N+1} , $(2N+1) \times (2N+1)$ matrix,

$$\mathbf{K}_{2N+1}(d, \Delta, \ell) = \begin{pmatrix} F_{0,0} & F_{1,0} & \dots & \dots & F_{2N+1,0} \\ F_{0,1} & F_{1,1} & \dots & \dots & \dots \\ \dots & \dots & F_{i,j} & \dots & \dots \\ \dots & \dots & \dots & \dots & \dots \\ F_{0,2N+1} & \dots & \dots & \dots & F_{2N+1,2N+1} \end{pmatrix}. \quad (3.17)$$

We can show that the condition for positivity discussed in [14], can be written in a more generic format, given by⁸,

$$g_i = \frac{|\mathbf{K}_i(d, \Delta, \ell)| |\mathbf{K}_{i-2}(d, \Delta, \ell)|}{|\mathbf{K}_{i-1}(d, \Delta, \ell)|^2} > 0, \quad (3.18)$$

where $|\mathbf{K}_i|$ gives the determinant of a $i \times i$ matrix and $|\mathbf{K}_i| = 1$ for $i < 0$. With this, as we have checked rigorously, all the positivity criterion discussed in [14] can be reproduced *viz.*

$$\begin{aligned} N = 0 : g_1 &= (G_{d,\Delta,\ell}^1)' > 0, \\ N = 1 : g_2 &= \left(\frac{(G_{d,\Delta,\ell}^2)'}{(G_{d,\Delta,\ell}^1)'} \right)' > 0, \quad g_3 = \left(\frac{\left(\frac{(G_{d,\Delta,\ell}^3)'}{(G_{d,\Delta,\ell}^1)'} \right)'}{\left(\frac{(G_{d,\Delta,\ell}^2)'}{(G_{d,\Delta,\ell}^1)'} \right)'} \right)' > 0 \end{aligned} \quad (3.19)$$

and so on.

⁸We have chosen the sign to be positive to concur with [14].

3.3 The crossing equation

So far we have discussed the notion of cyclic polytopes which is relatively simpler to compute analytically and associated with the notion of a collection of block vectors given in equation (3.6). However in the numerical bootstrap, the convex hull of vectors is defined with respect to the crossing equation and not directly with the blocks themselves. In order to connect the concept of *cyclic polytope* to bootstrap, we will need to put in the ingredient of “crossing” in the projective picture as well. Crossing in the diagonal limit reads

$$\mathcal{A}(z) = \left(\frac{z}{1-z} \right)^{2\Delta_\phi} \mathcal{A}(1-z). \quad (3.20)$$

This relates odd \mathcal{A}^{2n+1} in terms of the even ordered derivatives \mathcal{A}^{2n} . This in turn defines a hyperplane $\mathbf{X}[\Delta_\phi]$ which is a $(2N+2) \times (N+1)$ matrix in \mathbb{P}^{2N+1} . For example [14], for $N=2$ or $D=2N+1=5$,

$$\mathcal{A} = \begin{pmatrix} \mathcal{A}^0 \\ 4\Delta_\phi \mathcal{A}^0 \\ \mathcal{A}^2 \\ \frac{16}{3} (\Delta_\phi - 4\Delta_\phi^3) \mathcal{A}^0 + 4\Delta_\phi \mathcal{A}^2 \\ \mathcal{A}^4 \\ \frac{64}{15} \Delta_\phi (32\Delta_\phi^4 - 20\Delta_\phi^2 + 3) \mathcal{A}^0 - \frac{16}{3} \Delta_\phi (4\Delta_\phi^2 - 1) \mathcal{A}^2 + 4\Delta_\phi \mathcal{A}^4 \\ \vdots \end{pmatrix} \in \mathbb{P}^{2N+1}$$

and

$$\mathbf{X}[\Delta_\phi] = \begin{pmatrix} \mathcal{A}^0 & \mathcal{A}^2 & \mathcal{A}^4 \\ 1 & 0 & 0 \\ 4\Delta_\phi & 0 & 0 \\ 0 & 1 & 0 \\ \frac{16}{3} (\Delta_\phi - 4\Delta_\phi^3) & 4\Delta_\phi & 0 \\ 0 & 0 & 1 \\ \frac{64}{15} \Delta_\phi (32\Delta_\phi^4 - 20\Delta_\phi^2 + 3) & \frac{16}{3} (\Delta_\phi - 4\Delta_\phi^3) & 4\Delta_\phi \end{pmatrix}. \quad (3.21)$$

Now we have both ingredients for bootstrap in the projective picture.

- A convex hull of vectors built from $2N+2$ components of a block with a natural notion of ordering. This defines a *cyclic polytope* in \mathbb{P}^{2N+1} . Call this $\mathbf{U}[\Delta]$.
- A N -dimensional hyperplane $\mathbf{X}[\Delta_\phi]$.

The consistent solution of bootstrap entails finding $\mathbf{U}[\Delta] \cap \mathbf{X}[\Delta_\phi]$. The question now is given a $\mathbf{U}[\Delta]$, what are the conditions needed for the intersection with $\mathbf{X}[\Delta_\phi]$. As argued in [14], a k -plane intersects with a D -dimensional polytope with a $D-k$ face at a point given by,

$$\mathbf{v}_1 \langle \mathbf{v}_2, \mathbf{v}_3, \mathbf{v}_4, \dots, \mathbf{v}_{D-k}, \mathbf{X} \rangle - \mathbf{v}_2 \langle \mathbf{v}_1, \mathbf{v}_3, \mathbf{v}_4, \dots, \mathbf{v}_{D-k}, \mathbf{X} \rangle + \dots \quad (3.22)$$

For a point inside the polytope and satisfying the intersection property above,

$$\langle \mathbf{v}_2, \mathbf{v}_3, \mathbf{v}_4, \dots, \mathbf{v}_{D-k}, \mathbf{X} \rangle, -\langle \mathbf{v}_1, \mathbf{v}_3, \mathbf{v}_4, \dots, \mathbf{v}_{D-k}, \mathbf{X} \rangle, \langle \mathbf{v}_1, \mathbf{v}_2, \mathbf{v}_4, \dots, \mathbf{v}_{D-k}, \mathbf{X} \rangle, \dots, \quad \text{have same sign} \quad (3.23)$$

A further simplification occurs when one of the vertex vectors is the identity operator \mathbf{v}_0 or the infinity operator \mathbf{v}_∞ since this reduces the dimensionality of the problem. Another simplification is when projecting through specific planes obtained by performing a $GL(D+1)$ transformation,

$$\mathbf{X}' = \Lambda_{GL(D+1)} \cdot \mathbf{X}. \quad (3.24)$$

In terms of the intersection problem, $\langle \mathbf{X}', \dots \rangle$ reduces to a $D-k+1$ dimensional determinant, reducing the rank by $k-1$.

4 Positivity criterion for $\mathbf{U}[\Delta_i]$

Here we discuss the positivity criterion of $\mathbf{U}[\Delta_i]$ in diagonal limit. As mentioned in (3.18), a sufficient condition for positivity of the block vector is $g_i > 0$. Note however, that $g_i < 0$ does not necessarily mean that the cyclic polytope structure is absent; it simply means that in this case one needs to check (3.15) directly.

4.1 Scalar blocks

We plot below numerical evaluation of g_i for the scalar block. From figure [4] it is clear that:

- $g_i \rightarrow 2\sqrt{2} \forall i$ in the $\Delta \gg \frac{d-2}{2}$ limit.
- Some of the g_i 's are negative around $\Delta \sim \frac{d-2}{2}$.

The minima of the negative g_i 's shift upwards for increasing i ⁹. From $\Delta \gg \frac{d-2}{2}, \ell$ analysis we can track the Δ for which the minimum goes above the axis, which is indicated approximately in figure 4.

4.2 $\Delta \gg \frac{d-2}{2}, \ell$ limit analytic results

We can explain some of the features of g_i analytically by using the asymptotic blocks in section 2.2. For the scalar block we can parametrize the large Δ block as:

$$G_{d,\Delta,0}^{approx}(z) = e^{A(z)\Delta} B(z) \left(1 + \frac{c_1(z)}{\Delta} + \frac{c_2(z)}{\Delta^2} + O\left(\frac{1}{\Delta^3}\right) \right). \quad (4.1)$$

Using this and after coaxing mathematica a bit, we find

$$g_n = A'\left(\frac{1}{2}\right) - \frac{c'_1\left(\frac{1}{2}\right)}{\Delta^2} + 2 \frac{c_1\left(\frac{1}{2}\right)c'_1\left(\frac{1}{2}\right) - c'_2\left(\frac{1}{2}\right)}{\Delta^3} + \frac{(n-1)}{\Delta^3} \left(\frac{A'\left(\frac{1}{2}\right)c''_1\left(\frac{1}{2}\right) - A''\left(\frac{1}{2}\right)c'_1\left(\frac{1}{2}\right)}{A'\left(\frac{1}{2}\right)^2} \right) + O\left(\frac{1}{\Delta^4}\right). \quad (4.2)$$

⁹For $d=2$ we have not noticed any feature like this.

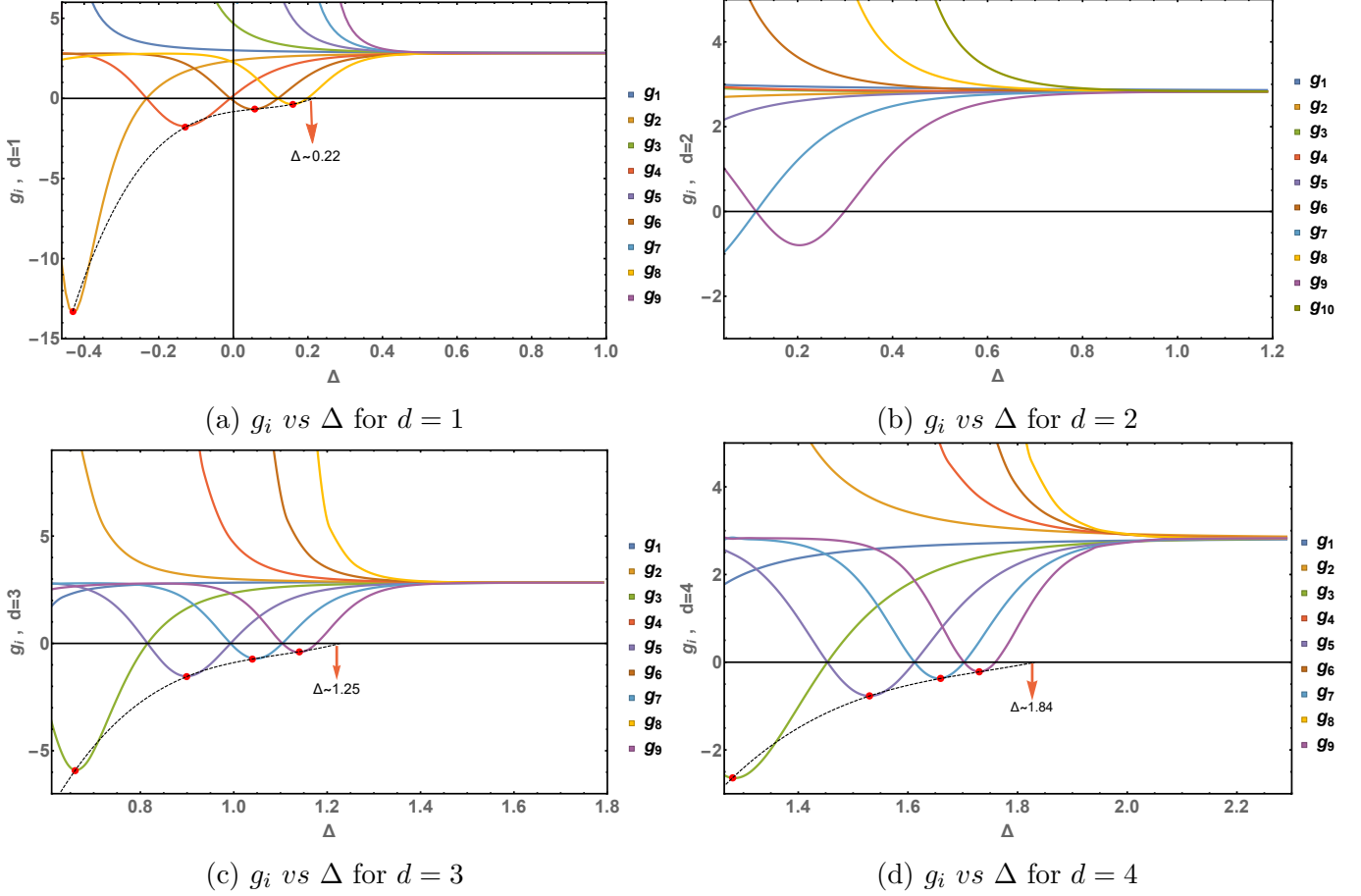


Figure 4: g_i vs Δ for scalar blocks for various d , plot range is $\Delta > \frac{d-2}{2}$. For $d = 1, 3, 4$ a trend is exhibited where it can be expected that eventually all g_i 's become positive for some Δ . For $d = 2$ such a trend does not exist and one is forced to check eq.(3.15) directly.

Notice that the correction begins at $1/\Delta^2$. This leads to the conclusion that the n -dependence is only through the last term in the above equation and the rest of the pieces are universal. Also observe that $B(z)$ in the block does not enter the final expression. We find

$$\begin{aligned}
 A'(\frac{1}{2}) &= 2\sqrt{2}, & c_1'(\frac{1}{2}) &= \frac{d(6-d)-4}{16\sqrt{2}}, & c_1''(\frac{1}{2}) &= \frac{5((d-6)d+4)}{16\sqrt{2}}, & A''(\frac{1}{2}) &= -2\sqrt{2}, \\
 c_2'(\frac{1}{2}) &= \frac{1}{512} \left(d \left(d \left(d \left(-2\sqrt{2}d + 3d + 32\sqrt{2} - 36 \right) - 136\sqrt{2} + 108 \right) + 32 \left(4\sqrt{2} + 3 \right) \right) - 16 \left(2\sqrt{2} + 9 \right) \right), .
 \end{aligned}
 \tag{4.3}$$

This explains why in the numerical plots, we found g_i 's approaching $2\sqrt{2} \approx 2.828$. Furthermore, since for non-zero spins, the leading order block is the same (up to some overall ℓ dependent factor which drops out in g_i), for non-zero spins too we will find the same result at leading order, namely $g_i \approx 2\sqrt{2}$. See Appendix A for derivation in general case. This essentially means:

For large Δ operators, the structure of the conformal block expansion is that of a cyclic polytope in any dimensions.

We then explicitly have for the $\ell = 0$ case

$$g_n = 2\sqrt{2} - \frac{d^2 - 6d + 4}{16\sqrt{2}\Delta^2} + \frac{24 - d(d(\sqrt{2}d - 6\sqrt{2} - 3) + 4\sqrt{2} + 30) + 3((d-6)d + 4)(n-1)}{32\Delta^3} + O\left(\frac{1}{\Delta^4}\right). \quad (4.4)$$

This means that the universal part is

$$g_n^{univ} = 2\sqrt{2} - \frac{d^2 - 6d + 4}{16\sqrt{2}\Delta^2} + \frac{24 - d(d(\sqrt{2}d - 6\sqrt{2} - 3) + 4\sqrt{2} + 30)}{32\Delta^3} + O\left(\frac{1}{\Delta^4}\right), \quad (4.5)$$

while the non-universal n -dependent part is

$$g_n^{non-univ} = (n-1) \times \frac{3((d-6)d + 4)}{32\Delta^3} + O\left(\frac{1}{\Delta^4}\right). \quad (4.6)$$

To be explicit

$$g_n|_{d=2} \approx 2.828 + \frac{0.177}{\Delta^2} + \frac{0.031[-12.686 - 12(n-1)]}{\Delta^3} + O(1/\Delta^4), \quad (4.7)$$

$$g_n|_{d=3} \approx 2.828 + \frac{0.221}{\Delta^2} + \frac{0.031[-17.787 - 15(n-1)]}{\Delta^3} + O(1/\Delta^4), \quad (4.8)$$

$$g_n|_{d=4} \approx 2.828 + \frac{0.177}{\Delta^2} + \frac{0.031[-25.373 - 12(n-1)]}{\Delta^3} + O(1/\Delta^4), \quad (4.9)$$

$$g_n|_{d=6} \approx 2.828 - \frac{0.177}{\Delta^2} + \frac{0.031[-81.941 + 12(n-1)]}{\Delta^3} + O(1/\Delta^4). \quad (4.10)$$

Notice that $c'_1(\frac{1}{2})$ changes sign at $d = 6$. Furthermore notice that $c'_1(\frac{1}{2})|_{d=2} = c'_1(\frac{1}{2})|_{d=4} = -c'_1(\frac{1}{2})|_{d=6} = \frac{1}{4\sqrt{2}}$. For $d \geq 6$, the leading $O(1/\Delta^2)$ correction is negative. Unless $\Delta \gg \frac{d-2}{2}$, the $O(1/\Delta^2)$ and $O(1/\Delta^3)$ terms are comparable. However, each can still be much smaller than the $2\sqrt{2}$ term. For instance for $d = 4, n = 1$ both $O(1/\Delta^2)$ and $O(1/\Delta^3)$ terms are < 0.1 .

4.3 Spin blocks

Similar analysis can be done for spin blocks for example we include here $\ell = 2$ for $d = 2$. The plots look similar for $d = 3, 4$ (Figure [5]).

Note that all the g_i 's are positive and almost $2\sqrt{2}$ for $\ell = 2$. The situation gets better for $\ell = 4, 6, 8$ and so on, since the unitary bounds are $\Delta \geq d + \ell - 2$ and the $\Delta \gg \frac{d-2}{2}, \ell$ analysis is valid here.

4.4 Weighted Minkowski sum

The Minkowski sum of set of vectors $X_i, i = 1, 2, \dots, n$, is defined as the set of vectors which can be written as the sum of a vector in X_i [17]

$$X_1 + X_2 + \dots + X_n := \{x_1 + x_2 + \dots + x_n | x_i \in X_i, \forall i\} \quad (4.11)$$

Note that Minkowski sum of polytopes is also a polytopes. Now if $P_i, i = 1, 2, \dots, n$ are polytopes

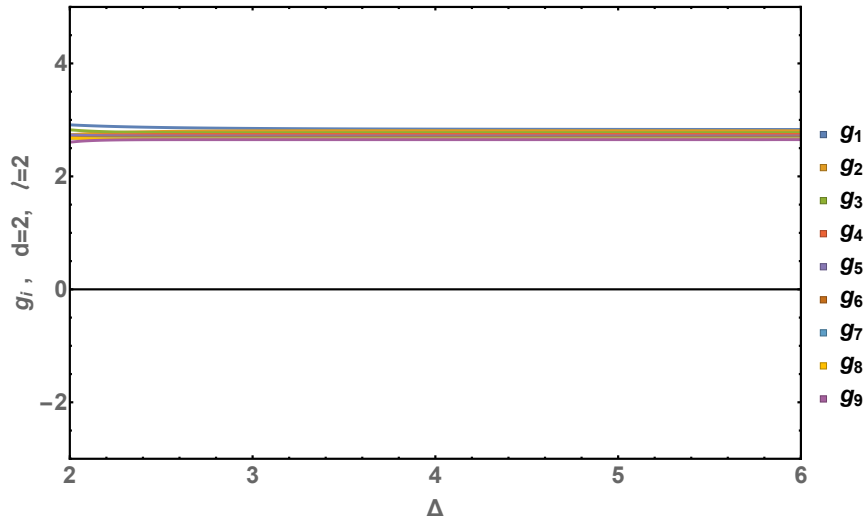


Figure 5: g_i vs Δ for $d = 2$, $\ell = 2$

in \mathbb{R}^d then their weighted Minkowski sum $P(\lambda_i)$ is defined as [17]

$$P(\lambda_i) = \lambda_1 P_1 + \lambda_2 P_2 + \dots + \lambda_n P_n; \lambda_i \geq 0, \forall i \quad (4.12)$$

As we mentioned the condition $g_i > 0$ is sufficient but not necessary. When $g_i < 0$ we resort to numerically checking $\langle \vec{G}_{d,\Delta_1,\ell_1}, \vec{G}_{d,\Delta_2,\ell_2}, \dots, \vec{G}_{d,\Delta_i,\ell_i} \rangle > 0$. We have found for each spin upto some small caveat pertaining to scalars close to the unitarity bound (see appendix (E)) that there is a cyclic polytope structure for unitary theories. After adding spin, the resulting polytope is $P(c_\ell) = c_0 P_0 + c_2 P_2 + c_4 P_4 + \dots$, where P_ℓ is the cyclic polytope structure following from the spin- ℓ block vectors. So we get the weighted Minkowski sum [17] of cyclic polytopes which itself is not necessarily a cyclic polytope (as we explicitly demonstrate in the Appendix B). However if we work with the approximate blocks, as we have shown above, the result is again a cyclic polytope irrespective of spin sum.

This is the motivation for looking at the large Δ limit in order to derive some intuition about what the cyclic polytope picture can teach us about bootstrap.

5 $N = 1$: Bounds on leading operator

A general constraint arising from $\mathbf{U}\{\Delta\} \cap \mathbf{X}[\Delta_\phi]$ is then given by a $2n \times 2n$ matrix whose last n entries are the columns from the basis vectors of the unitary polytope. As a simple example, we can demonstrate some generalizations of the bounds for $N = 1$ in (projecting through identity) in [14, eq.

7.9] for higher dimensions. The crossing plane \mathbf{X} is one-dimensional,

$$\mathbf{X} = \begin{pmatrix} \mathcal{A}^0 & \mathcal{A}^2 \\ 1 & 0 \\ 4\Delta_\phi & 0 \\ 0 & 0 \\ \frac{16}{3}(\Delta_\phi - 4\Delta_\phi^3) & 4\Delta_\phi \end{pmatrix}. \quad (5.1)$$

The polytope is 3-dimensional. The facets can be found by using (3.14)

$$(\mathbf{G}_{d,\Delta_0,0}, \mathbf{G}_{d,\Delta_i,0}, \mathbf{G}_{d,\Delta_{i+1},0}), \quad (\mathbf{G}_{d,\Delta_i,0}, \mathbf{G}_{d,\Delta_{i+1},0}, \mathbf{G}_{d,\Delta_\infty,0}) \quad (5.2)$$

Here the identity operator $\mathbf{G}_{d,\Delta_0,0} = (1, 0, 0, 0)$ and ∞ is $\mathbf{G}_{d,\Delta_\infty,0} = (0, 0, 0, 1)$. No other operator in between Δ_i and Δ_{i+1} and we order them as $\Delta_i < \Delta_{i+1}$. The crossing plane \mathbf{X} intersects with the facets if and only if equation (3.23) is satisfied. As we mentioned earlier it is sometimes simple and useful to take the projection through some special point [14].

5.1 Projection through identity

We project our three-dimensional cyclic polytope through the identity $\mathbf{G}_{d,\Delta_0,\ell_0} = (1, 0, 0, 0)$. As mentioned in [14] that the necessary conditions one can get by forcing $\langle \mathbf{X}, 0, \Delta \rangle$ to be zero. The crossing plane intersects the unitary cyclic polytope at two points which are given by the two solutions Δ_-, Δ_+ of

$$\langle \mathbf{X}, 0, \Delta \rangle = 0. \quad (5.3)$$

This tells us that there must exist at least one operator with dimension Δ such that

$$\Delta_- < \Delta < \Delta_+. \quad (5.4)$$

This also implies that the gap between the identity and the leading operator has to be smaller than Δ_+ . Below we tabulate Δ_+, Δ_- for various Δ_ϕ :

Δ_ϕ	Δ_+	Δ_-
0.1	1.29591	0.111592
0.2	1.58656	0.237821
0.3	1.87438	0.371258
0.4	2.16053	0.508445
0.5	2.44564	0.647694
0.6	2.73006	0.788127

Table 1: List of Δ_+, Δ_- for various Δ_ϕ , $d = 1$

Δ_ϕ	Δ_+	Δ_-
0.1	1.20812	0.120067
0.125	1.2826	0.151471
0.2	1.50422	0.247921
0.3	1.79662	0.380248
0.4	2.08665	0.515341
0.5	2.37507	0.652232

Table 2: List of Δ_+, Δ_- for various Δ_ϕ , $d = 2$

It is possible to further constrain the Δ_+ and Δ_- including spin analysis from the technique of $N = 2$ analysis given in section (6). We will study this in detail in a forthcoming publication [21]. In

Δ_ϕ	Δ_+	Δ_-
0.5	2.26058	0.697759
0.518	2.31459	0.715473
0.6	2.55882	0.807958
0.7	2.85357	0.934263
0.8	3.14593	1.06673
0.9	3.43657	1.20214
1.	3.72592	1.33921

Table 3: List of Δ_+, Δ_- for various Δ_ϕ , $d = 3$

Δ_ϕ	Δ_+	Δ_-
1.	3.61311	1.3043
1.2	4.20493	1.58012
1.4	4.789	1.85969
1.6	5.36839	2.14053
1.8	5.94472	2.42204
1.9	6.23204	2.56297
2.	6.51892	2.70398

Table 4: List of Δ_+, Δ_- for various Δ_ϕ , $d = 4$

appendix (D) we have made a preliminary study of the effects of adding spin to the analysis of bound on the dimension of the leading scalar.

5.2 Δ_+ and Δ_- for large Δ_ϕ

Using eq (2.1) with the approximations of the ${}_3F_2$ given in section 2.2,¹⁰ we can find analytic solutions for Δ_+ and Δ_- for large Δ_ϕ :

$$\begin{aligned}
\Delta_+ &= 2\sqrt{2}\Delta_\phi + \frac{(2\sqrt{2}-3)d+6}{4\sqrt{2}} + \frac{12-d(d+6)}{128\sqrt{2}\Delta_\phi} - \frac{3(d(d(d+2)-44)+88)}{2048\sqrt{2}\Delta_\phi^2} \\
&\quad + \frac{d(-d(d+6)(37d-282)-7392)+15216}{131072\sqrt{2}\Delta_\phi^3} + O\left(\frac{1}{\Delta_\phi^4}\right) \\
\Delta_- &= \sqrt{2}\Delta_\phi + \frac{1}{8}(4-3\sqrt{2})d - \frac{(d-6)d+12}{64\sqrt{2}\Delta_\phi} - \frac{3((d-4)^2d-32)}{512\sqrt{2}\Delta_\phi^2} \\
&\quad + \frac{d((372-37d)d-1188)+480-1680}{16384\sqrt{2}\Delta_\phi^3} + O\left(\frac{1}{\Delta_\phi^4}\right)
\end{aligned} \tag{5.5}$$

This formula is even very good approximation for $\Delta_\phi > 1$. For comparison we give a plot for Δ_+ and Δ_- vs Δ_ϕ calculated using exact block and eq (5.5).

¹⁰For $O(\frac{1}{\Delta_\phi^n})$ one has to add $O(\frac{1}{\Delta_\phi^n})$ corrections to eq (2.6) using [18].

We can also expand around $\Delta_\Phi = \Delta_\phi + a$

$$\begin{aligned}
\Delta_+ &= 2\sqrt{2}\Delta_\Phi + \frac{1}{8} \left(-16\sqrt{2}a + (4 - 3\sqrt{2})d + 6\sqrt{2} \right) + \frac{12 - d(d+6)}{128\sqrt{2}\Delta_\Phi} \\
&\quad + \frac{-16a(d(d+6) - 12) - 3(d(d(d+2) - 44) + 88)}{2048\sqrt{2}\Delta_\Phi^2} \\
&\quad + \frac{-1024a^2(d(d+6) - 12) - 384a(d(d(d+2) - 44) + 88) + d(-d(d+6)(37d - 282) - 7392) + 15216}{131072\sqrt{2}\Delta_\Phi^3} \\
&\quad + O\left(\frac{1}{\Delta_\Phi^4}\right) \\
\Delta_- &= \sqrt{2}\Delta_\Phi + \left(\frac{1}{8} \left(4 - 3\sqrt{2} \right) d - \sqrt{2}a \right) - \frac{(d-6)d + 12}{64\sqrt{2}\Delta_\Phi} + \frac{-8a((d-6)d + 12) - 3((d-4)^2d - 32)}{512\sqrt{2}\Delta_\Phi^2} \\
&\quad + \frac{-256a^2((d-6)d + 12) - 192a((d-4)^2d - 32) + d(d((372 - 37d)d - 1188) + 480) - 1680}{16384\sqrt{2}\Delta_\Phi^3} \\
&\quad + O\left(\frac{1}{\Delta_\Phi^4}\right)
\end{aligned} \tag{5.6}$$

One can easily see from Figure (6) that eq (5.6) with $a = 0$ i.e 5.5 is very good approximation for $\Delta_\phi > 1$, while it deviates a lot from the exact numbers for $\Delta_\phi < 1$. Also 5.6 is very good approximation even for $\Delta_\phi < 1$ for the choice of $a = 1$. One can optimize the value of a for better numerical agreement for $\Delta_\phi < 1$, which we have not done here.

5.3 Interpretation of Δ_+ and Δ_- from numerical bootstrap

From crossing symmetry equation (1.4, 3.20) in diagonal limit we have,

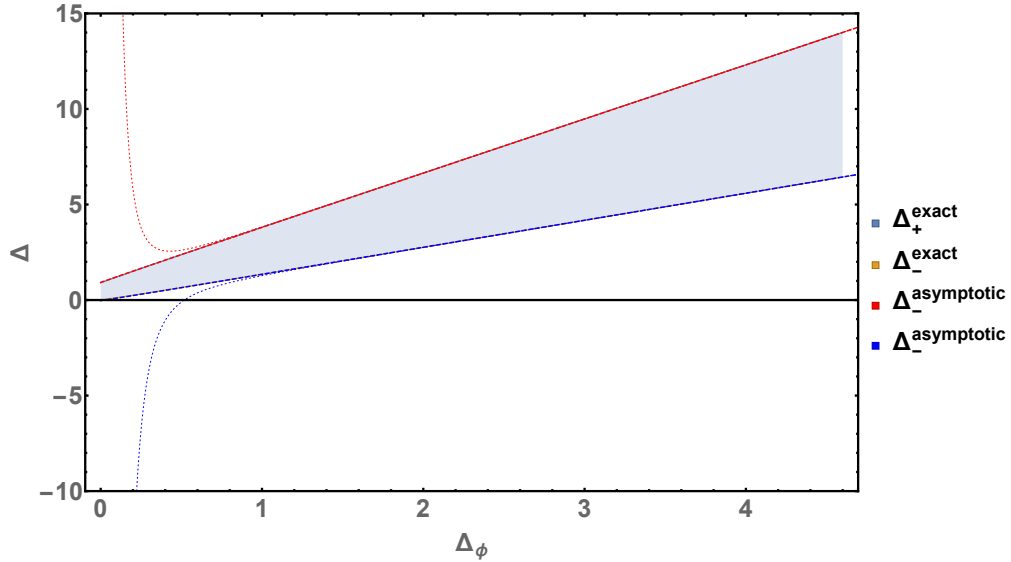
$$\sum_{\Delta, \ell} C_{\Delta, \ell} \mathcal{F}_{d, \Delta, \ell}(z) = 1, \tag{5.7}$$

where $\mathcal{F}_{d, \Delta, \ell}(z)$ is given in equation (3.1). We can write

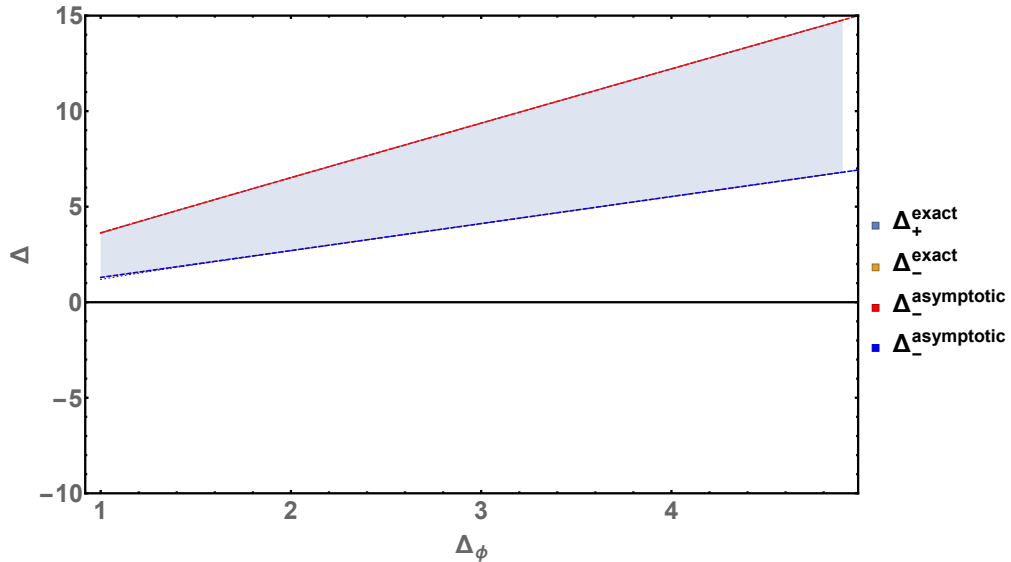
$$\sum_{\Delta, \ell} C_{\Delta, \ell} \partial_z^2 \mathcal{F}_{d, \Delta, \ell}(z)|_{z=1/2} = 0, \tag{5.8}$$

From figure (8), it is clear that $\partial_z^2 \mathcal{F}_{d, \Delta, 0}(z)|_{z=1/2}$ changes its sign at indicated values. At least there should be one operator below Δ_+ (the larger value) in order to satisfy equation (5.8).

A peculiar feature that is captured by both the analysis we are doing in this section as well as the polytope method, is that there is a third root of the $N = 1$ determinant (or equivalently $\partial_z^2 \mathcal{F}_{d, \Delta, 0}(z)|_{z=\frac{1}{2}}$) which allows for a small region $\frac{d-2}{2} < \Delta < \Delta_*$ close to the unitarity bound as an allowed region. However, it seems to us that this is somewhat artificial and we will not comment on this further. The main point is that there could always be operators below Δ_- as well, but there must be at least one operator (which need not be the leading scalar operator in the OPE which happens if



(a) Δ_+, Δ_- vs Δ_ϕ for $d = 2$



(b) Δ_+, Δ_- vs Δ_ϕ for $d = 4$

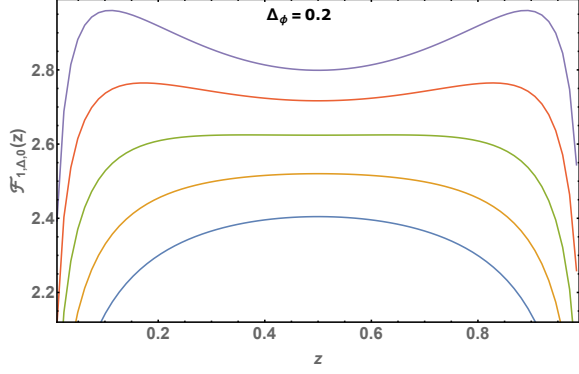
Figure 6: Solid lines represent Δ_+, Δ_- calculated using exact block while dashed lines are eq (5.6), dashed lines represent $a = 1$ and dotted are $a = 0$. We have included here only $d = 2, 4$ but the feature is similar for $d = 1, 3$.

there are operators¹¹ $\Delta < \Delta_-$) such that $\Delta_- < \Delta < \Delta_+$ for there to be any chance for a solution.

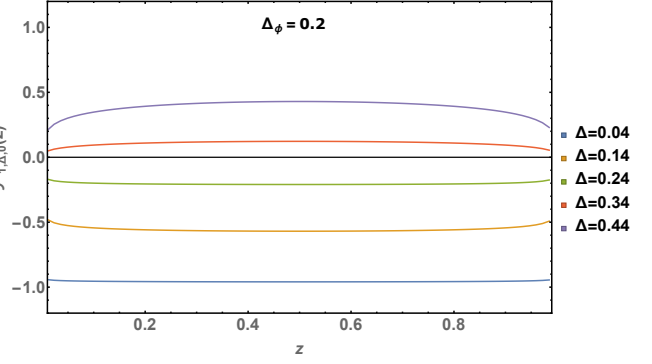
6 $N = 2$: Constraints on the first two primary operators

In this section, we consider $N = 2$ *i.e.*, the 5-dimensional polytope. The crossing plane is given in equation (3.21) and the boundaries can be found using 3.14. As before, for simplicity and usefulness

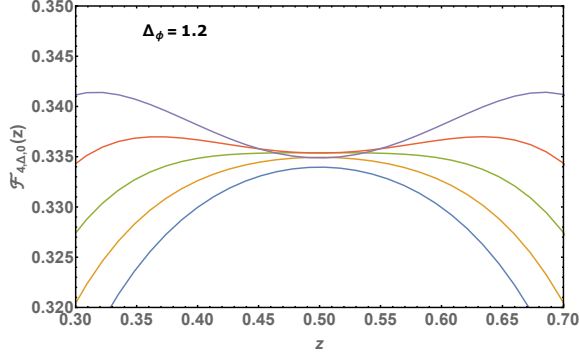
¹¹A simple example is the case where in a free theory in $d = 4$ we have the external operator to be ϕ^2 so that the leading scalar operator is ϕ^2 itself. From table (4), it is clear that since $\Delta_{\phi^2} = 2$ we have $\Delta_{\phi^2} < \Delta_-$.



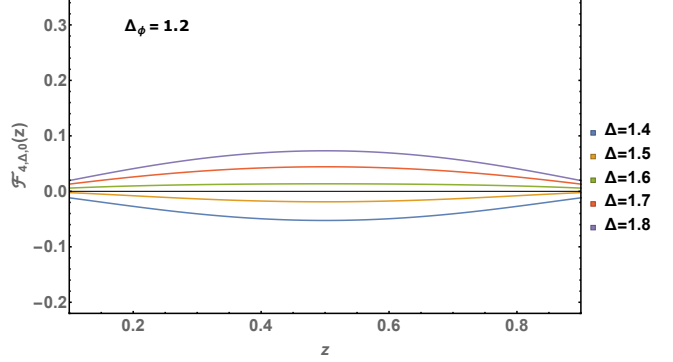
(a) $\mathcal{F}_{d,\Delta,0}(z)$ vs z for $d = 1$



(b) $\mathcal{F}_{d,\Delta,0}(z)$ vs z for $d = 1$

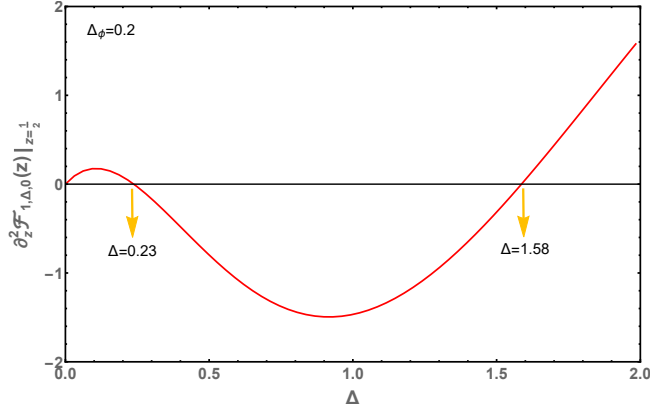


(c) $\mathcal{F}_{d,\Delta,0}(z)$ vs z for $d = 4$

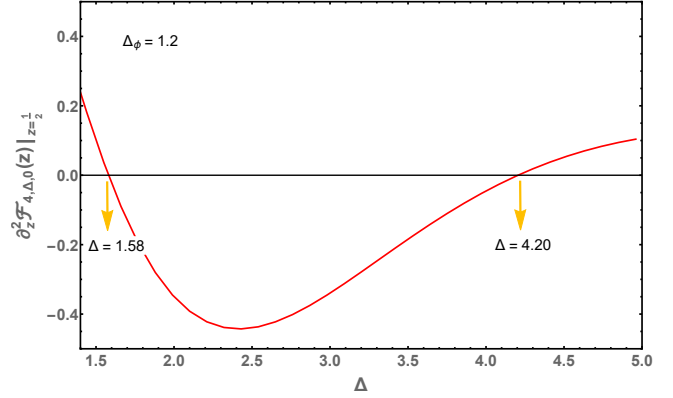


(d) $\mathcal{F}_{d,\Delta,\ell}(z)$ vs z for $d = 4$

Figure 7: $\mathcal{F}_{d,\Delta,0}(z)$ vs z to show Δ_+ and Δ_- from numerical bootstrap



(a) $\partial_z^2 \mathcal{F}_{d,\Delta,0}(z)|_{z=1/2}$ vs Δ for $d = 1$



(b) $\partial_z^2 \mathcal{F}_{d,\Delta,0}(z)|_{z=1/2}$ vs Δ for $d = 4$

Figure 8: $\partial_z^2 \mathcal{F}_{d,\Delta,0}(z)|_{z=1/2}$ vs Δ . See table 1 and table 4 for values of Δ_+ and Δ_- . The indicated values in the plot is exactly matched with the value given in the tables

we will view the geometry projected through identity [14]. The constraints for the first two operators Δ_1, Δ_2 is as follows. For $\Delta_1 < \Delta_-$ we should have $\Delta_2 < \Delta_+$, otherwise there will be no operators between (Δ_-, Δ_+) as we observed in the $N = 1$ case. And also $\Delta_1 > \Delta_+$ is not allowed if Δ_1 is the leading operator. As explained in [14], the necessary conditions one would obtain from the observation that for $\Delta_- < \Delta_1 < \Delta_+$, Δ_2 must be below the curve $\langle \mathbf{X}, 0, \Delta_1, \Delta_2 \rangle = 0$ (see figure (9)), otherwise

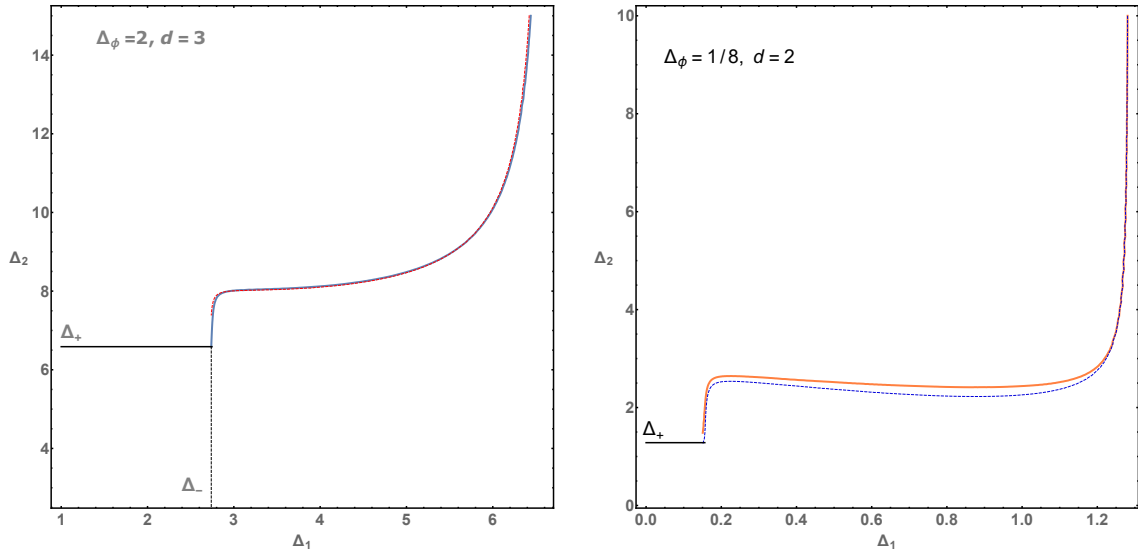


Figure 9: (a) Blue line is using exact scalar blocks and the red dashed line is using asymptotic scalar blocks. (b) Orange line is using spin-2 block for Δ_2 and blue dashed line is using scalar block for Δ_2 .

3.23 is not satisfied. Explicitly

$$\langle \mathbf{X}, 0, \Delta_1, \Delta_2 \rangle = \det \begin{pmatrix} 1 & 0 & 0 & 1 & 1 & 1 \\ 4\Delta\phi & 0 & 0 & 0 & G_{d,\Delta_1,0}^{(1)} & G_{d,\Delta_2,0}^{(1)} \\ 0 & 1 & 0 & 0 & G_{d,\Delta_1,0}^{(2)} & G_{d,\Delta_2,0}^{(2)} \\ \frac{16}{3}(\Delta\phi - 4\Delta\phi^3) & 4\Delta\phi & 0 & 0 & G_{d,\Delta_1,0}^{(3)} & G_{d,\Delta_2,0}^{(3)} \\ 0 & 0 & 0 & 1 & 0 & G_{d,\Delta_1,0}^{(4)} & G_{d,\Delta_2,0}^{(4)} \\ \frac{64}{15}\Delta\phi(32\Delta\phi^4 - 20\Delta\phi^2 + 3) & \frac{4}{15}\Delta\phi(20 - 80\Delta\phi^2) & 4\Delta\phi & 0 & G_{d,\Delta_1,0}^{(5)} & G_{d,\Delta_2,0}^{(5)} \end{pmatrix}. \quad (6.1)$$

We show in fig. 9 how the curve $\langle \mathbf{X}, 0, \Delta_1, \Delta_2 \rangle = 0$ changes if we put the second operator to be one with spin (there is an assumed ordering and in this instance we are assuming that the second operator is one that carries spin, assuming that the cyclic polytope structure is preserved). In figure (9.a) we have taken $\Delta_\phi = 2$, $d = 3$, both Δ_2 and Δ_1 blocks are taken to be scalar block for this case. In figure (9.b), we have taken the 2d Ising model $\Delta_\phi = \frac{1}{8}$ and used the spin $\ell = 2$ block for the operator Δ_2 i.e we used $\mathbf{G}_{2,\Delta_2,2}$ instead of $\mathbf{G}_{2,\Delta_2,0}$. One can see the plot is only slightly different if one uses scalar block i.e $\mathbf{G}_{2,\Delta_2,0}$ for the operator Δ_2 . Had the Δ_2 operator been a scalar (say by demand) in this case, we would be forced to conclude that $\Delta_2 = 4$ is not allowed thereby leading to a contradiction with the known result. Thankfully, from the plot, the spin-2 bound allows for $\Delta = 2$ which is the stress tensor and should be treated as the second operator.

7 Kink from positive geometry

In this section we will explain how the red line in fig.1 was obtained. We consider 10 scalar operators Δ_i where Δ_0 is the identity operator and Δ_9 is the infinity vector. $\Delta_1 = \Delta_S$ and $\Delta_i, i \geq 2$ are chosen

randomly to be above¹² Δ_S . The intersection conditions eq.(3.23) are now checked. For $N = 1$ we find essentially the same results as obtained in sec. 5.1. However for $N = 2$ the result is different. We find that there is a kink type feature in the plot as in fig.1. In fig.1 below the red line, there is always at least some region where the intersection conditions are satisfied (but not above the line). So why does a kink arise?

For concreteness, let us examine the signs of the determinants arising from the intersection of the crossing plane with $(\mathbf{v}_0, \mathbf{v}_1, \mathbf{v}_8, \mathbf{v}_9)$. While $det_1 = \langle \mathbf{X}, \mathbf{v}_1, \mathbf{v}_8, \mathbf{v}_9 \rangle$, $det_2 = \langle \mathbf{v}_0, \mathbf{X}, \mathbf{v}_8, \mathbf{v}_9 \rangle$ are negative in the range displayed above, $det_3 = \langle \mathbf{v}_0, \mathbf{v}_1, \mathbf{X}, \mathbf{v}_9 \rangle$ and $det_4 = \langle \mathbf{v}_0, \mathbf{v}_1, \mathbf{v}_8, \mathbf{X} \rangle$ are not always negative. The plots in fig.11 are for det_3, det_4 . Above $\Delta_\phi \approx 0.08$, there is a small region below $\Delta_S \approx 1.178$ where both are negative but below $\Delta_\phi \approx 0.08$, the region where they are both negative jumps further left giving rise to the kink in fig.1.

In other dimensions, there are also kinks. For $d = 1$, the kink appears $\Delta \sim 0$, for $d = 3$, the kink appears around $\Delta \sim 0.26$ and for $d = 4$, it appears near $\Delta \sim 0.5$. The latter two are for non-unitary operators and hence we will not consider them further. When we put in operators with spin, while the qualitative features not affected, the exact location of the kink moves around slightly. However, we have not investigated this in detail as the faces in this case are those of the weighted Minkowski sum which is not that of a cyclic polytope necessarily. If we repeated this analysis with the asymptotic blocks, the kink is no longer as sharp as in fig.1. We leave the search for an analytic (asymptotic) equation for the kink via this approach for future work. This is not impossible: a strategy would be to examine carefully the location of the largest zeroes in det_3, det_4 by plugging in the asymptotic blocks and studying analytically when they cross each other. We have looked at this problem and our preliminary analysis can be found in appendix C. Another question that we leave for the future is exploring higher N constraints to see what effect it has on the kink.

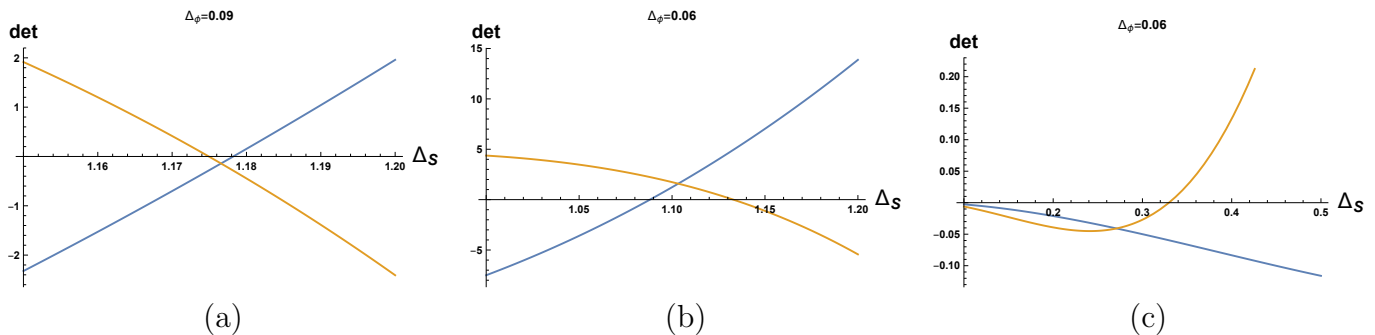


Figure 10: Plots of det_3, det_4 as a function of Δ_S . The blue plot is for det_3 while the orange plot is for det_4 .

¹²For definiteness $\Delta_2 = \Delta_S + 0.02, \Delta_3 = \Delta_S + 0.12, \Delta_4 = \Delta_S + 0.22, \Delta_5 = \Delta_S + 0.32, \Delta_6 = \Delta_S + 1.42, \Delta_7 = \Delta_S + 1.52, \Delta_8 = \Delta_S + 2.62$ Changing these spacings do not affect the qualitative features of the plot.

8 Discussion

In this paper we have extended the work of [14] in several directions. First, we have considered the diagonal limit in arbitrary dimensions and have shown that in the large Δ limit, even in the presence of spin, the geometric structure of the expansion in terms of the diagonal blocks of [15] is that of a cyclic polytope. We presented various analytic results and also initiated a comparison between the usual numerical bootstrap of [1] and the positive geometry constraints. We conclude with some possible future directions:

- One can consider more systematically the higher N generalizations of the analysis presented in this paper, especially with the kink picture, also including the contributions from higher spins. This can be done irrespective of the polytope being a cyclic one. It will also be interesting to see if there is some systematic classification of the facets of the weighted Minkowski sum that we found in this paper. More ambitiously, one can also try to develop a systematic asymptotic (in $1/\Delta$) analytic equation for the kink—in our context we have made a preliminary attempt in appendix C.
- There is still work to be done in order to connect this geometric picture to the usual numerical bootstrap. The main direction to proceed from here is the generalization of the geometric approach to the non-diagonal case. The usual numerical bootstrap takes the input of both the dimension and spin for the generic off-diagonal blocks (*i.e* the block is a function of both z and \bar{z}). In that sense the bound obtained from numerical bootstrap is more constraining. As already pointed out in [14], for the off-diagonal case, the simple picture of the polytopes does not apply and it generalizes to tensor products of the simple polytope picture we have handled so far. It would be interesting to see what the generalization has in store for us and how much can still be done analytically using the tensor product of (cyclic) polytopes.
- We can also consider the alternate formulation of the bootstrap in [7–12] using the *Polyakov blocks* which are manifestly crossing symmetric and ask about the *OPE consistency* in terms of the geometric picture. In that case the consistency conditions arise by demanding the absence of certain spurious poles. These conditions in the diagonal limit schematically read

$$\sum_{\Delta, \ell} C_{\Delta, \ell} q_{\Delta, \Delta, \ell}(s) = 0, \quad s = \Delta_\phi + n$$

where s is Mellin variable and n is an integer. Thus they are similar to the $m > 0$ conditions listed in eq.(3.3). This would be the natural starting point for a linear programming based approach using Polyakov blocks. It remains to be seen if Polyakov block expansion and cyclic polytopes are in any sense related.

Acknowledgments

We thank Kausik Ghosh, Yu-tin Huang and Slava Rychkov for discussions and correspondence. A.S. acknowledges support from a DST Swarnajayanti Fellowship Award DST/SJF/PSA-01/2013-14.

A Derivation of $g_i \approx 2\sqrt{2}$ in $\Delta \gg \frac{d-2}{2}, \ell$ limit, general case.

Using the large Δ limit of the diagonal blocks in (2.6), we can grind out the positivity criterion analytically at least in the $\Delta \gg \frac{d-2}{2}, \ell$ limit. Step-wise,

$$\left. \frac{\partial_z^m G_{d,\Delta,\ell}(z)}{m!} \right|_{z=\frac{1}{2}} = \frac{\sqrt{\pi} \left(2 + \frac{3}{\sqrt{2}}\right)^{d/2} (12\sqrt{2} + 17)^{-\frac{\Delta}{2}} \Delta^m 2^{-2d+2\Delta+\frac{3m}{2}+3} \Gamma(d+\ell-2)}{\Gamma\left(\frac{d-1}{2}\right) (2)_{m-1} \Gamma\left(\frac{d}{2} + \ell - 1\right)} \left[1 + O\left(\frac{1}{\Delta}\right)\right], \quad (\text{A.1})$$

are the block vectors. Now using Leibniz theorem we can calculate $F_{m,n} = \partial_\Delta^n \left(\frac{\partial_z^m G_{d,\Delta,\ell}(z)}{m!}\right)$, in a simple closed form expression,

$$F_{m,n} = \frac{\sqrt{\pi} \left(2 + \frac{3}{\sqrt{2}}\right)^{d/2} (12 - 8\sqrt{2})^\Delta 2^{-2d+\frac{3m}{2}+3} \Delta^m (-\Delta)^{-n} \Gamma(d+\ell-2)}{\Gamma\left(\frac{d-1}{2}\right) (2)_{m-1} \Gamma\left(\frac{d}{2} + \ell - 1\right)} U\left(-n, m-n+1, -\Delta \log\left(12 - 8\sqrt{2}\right)\right) \left(1 + O\left(\frac{1}{\Delta}\right)\right) \quad (\text{A.2})$$

U is HypergeometricU or Tricomi confluent hypergeometric function. Some of the $\mathbf{K}_{2N+1}(d, \Delta, \ell)$ are,

$$\begin{aligned} |\mathbf{K}_0(d, \Delta, \ell)| &= \frac{\sqrt{\pi} 2^{3-2d} \left(2 + \frac{3}{\sqrt{2}}\right)^{d/2} (12 - 8\sqrt{2})^\Delta \Gamma(d+\ell-2)}{\Gamma\left(\frac{d-1}{2}\right) \Gamma\left(\frac{d}{2} + \ell - 1\right)} + O(\Delta^{-1}), \\ |\mathbf{K}_1(d, \Delta, \ell)| &= \frac{\pi 2^{\frac{15}{2}-4d} \left(2 + \frac{3}{\sqrt{2}}\right)^d (12 - 8\sqrt{2})^{2\Delta} \Gamma(d+\ell-2)^2}{\Gamma\left(\frac{d-1}{2}\right)^2 \Gamma\left(\frac{d}{2} + \ell - 1\right)^2} + O(\Delta^{-1}), \\ |\mathbf{K}_2(d, \Delta, \ell)| &= \frac{\pi^{3/2} 2^{\frac{27}{2}-6d} \left(2 + \frac{3}{\sqrt{2}}\right)^{\frac{3d}{2}} (12 - 8\sqrt{2})^{3\Delta} \Gamma(d+\ell-2)^3}{\Gamma\left(\frac{d-1}{2}\right)^3 \Gamma\left(\frac{d}{2} + \ell - 1\right)^3} + O(\Delta^{-1}). \end{aligned} \quad (\text{A.3})$$

For the leading order $|\mathbf{K}_i|$, a general formula for large Δ , then looks like,

$$|\mathbf{K}_i(d, \Delta, \ell)| = \frac{\pi^{\frac{i+1}{2}} 2^{\frac{3}{4}(i+1)(i+4)-2d(i+1)} \left(2 + \frac{3}{\sqrt{2}}\right)^{\frac{1}{2}d(i+1)} (12 - 8\sqrt{2})^{\Delta(i+1)} \Gamma(d+\ell-2)^{i+1}}{\Gamma\left(\frac{d-1}{2}\right)^{i+1} \Gamma\left(\frac{d}{2} + \ell - 1\right)^{i+1}} + O(\Delta^{-1}). \quad (\text{A.4})$$

Now using eq.(3.18) one can easily compute g_i analytically, to obtain

$$g_i \approx 2\sqrt{2} : \quad \forall i, \quad \Delta \gg \frac{d-2}{2}, \ell. \quad (\text{A.5})$$

All the g_i 's are positive for large Δ for any d and any ℓ . Therefore we conclude that unitary polytope $\mathbf{U}\{\Delta_i\}$ is a cyclic polytope in the limit $\Delta \gg \frac{d-2}{2}, \ell$

B Some examples using known theories

Here we will explicitly check eq.(3.15) for some physical theories for e.g. 2D and 3D Ising model, taking the first few operators in the spectrum.

B.1 2d Ising model

The first few operators in increasing order of Δ for the 2d Ising model are given by (see 2nd reference in [3])

$$\begin{aligned} \Delta_1 = 1, \Delta_2 = 2, \Delta_3 = 4, \Delta_4 = 4, \Delta_5 = 5, \Delta_6 = 6, \Delta_7 = 6, \Delta_8 = 7, \Delta_9 = 8, \Delta_{10} = 8 \\ \ell_1 = 0, \ell_2 = 2, \ell_3 = 0, \ell_4 = 4, \ell_5 = 4, \ell_6 = 2, \ell_7 = 6, \ell_8 = 6, \ell_9 = 0, \ell_{10} = 4. \end{aligned} \quad (\text{B.1})$$

i	$\langle \vec{G}_{d,\Delta_1,\ell_1}, \vec{G}_{d,\Delta_2,\ell_2}, \dots, \vec{G}_{d,\Delta_i,\ell_i} \rangle$	i	$\langle \vec{G}_{d,\Delta_1,\ell_1}, \vec{G}_{d,\Delta_2,\ell_2}, \dots, \vec{G}_{d,\Delta_i,\ell_i} \rangle$
1	2.9139	1	4.17363
2	22.6087	2	78.5859
3	2162.57	3	2420.5
4	-15191.9	4	249319.
5	1.53684×10^6	5	2.51128×10^7
6	-5.23824×10^7	6	3.85515×10^9
7	-1.85813×10^8	7	1.15493×10^{12}
8	-8.39807×10^{10}	8	-9.71096×10^{12}
9	-1.68276×10^{12}	9	6.31945×10^{14}

Table 5: Left: Determinants of first few operators of 2D Ising model using equation (2.1), spectrum (B.1) and Right: determinants of first few operators of 3D Ising model using 2.1, spectrum (B.2).

Various facets are given below table (6) for the above spectrum for $D = 2N = 4$ i.e. even dimensional polytopes. Notice in table (6) that **facet=1,3,6,8,11,12,13,16,17** are not part of a cyclic polytopes.

B.2 3d Ising model

Similarly for the 3d Ising model [20]

$$\begin{aligned} \Delta_1 = 1.41263, \Delta_2 = 3, \Delta_3 = 3.82968, \Delta_4 = 5.02267, \Delta_5 = 5.5091, \\ \Delta_6 = 6.42065, \Delta_7 = 6.8956, \Delta_8 = 7.0758, \Delta_9 = 7.2535 \\ \ell_1 = 0, \ell_2 = 2, \ell_3 = 0, \ell_4 = 4, \ell_5 = 2, \ell_6 = 4, \ell_7 = 0, \ell_8 = 2, \ell_9 = 0. \end{aligned} \quad (\text{B.2})$$

B.3 Different ordering of combinations of Δ and ℓ

In above discussions we have ordered the spectrum in increasing value of Δ . It may be possible that ordering in terms of say twist $\Delta - \ell$, will lead to a cyclic polytope even for $O(1)$ values of Δ . In this

facet-1	$\mathbf{G}_{d,\Delta_0,\ell_0}$	$\mathbf{G}_{d,\Delta_1,\ell_1}$	$\mathbf{G}_{d,\Delta_2,\ell_2}$	$\mathbf{G}_{d,\Delta_4,\ell_4}$
facet-2	$\mathbf{G}_{d,\Delta_0,\ell_0}$	$\mathbf{G}_{d,\Delta_1,\ell_1}$	$\mathbf{G}_{d,\Delta_4,\ell_4}$	$\mathbf{G}_{d,\Delta_5,\ell_5}$
facet-3	$\mathbf{G}_{d,\Delta_0,\ell_0}$	$\mathbf{G}_{d,\Delta_1,\ell_1}$	$\mathbf{G}_{d,\Delta_5,\ell_5}$	$\mathbf{G}_{d,\Delta_7,\ell_7}$
facet-4	$\mathbf{G}_{d,\Delta_0,\ell_0}$	$\mathbf{G}_{d,\Delta_1,\ell_1}$	$\mathbf{G}_{d,\Delta_7,\ell_7}$	$\mathbf{G}_{d,\Delta_8,\ell_8}$
facet-5	$\mathbf{G}_{d,\Delta_0,\ell_0}$	$\mathbf{G}_{d,\Delta_1,\ell_1}$	$\mathbf{G}_{d,\Delta_8,\ell_8}$	$\mathbf{G}_{d,\Delta_9,\ell_9}$
facet-6	$\mathbf{G}_{d,\Delta_0,\ell_0}$	$\mathbf{G}_{d,\Delta_5,\ell_5}$	$\mathbf{G}_{d,\Delta_6,\ell_6}$	$\mathbf{G}_{d,\Delta_7,\ell_7}$
facet-7	$\mathbf{G}_{d,\Delta_1,\ell_1}$	$\mathbf{G}_{d,\Delta_2,\ell_2}$	$\mathbf{G}_{d,\Delta_4,\ell_4}$	$\mathbf{G}_{d,\Delta_5,\ell_5}$
facet-8	$\mathbf{G}_{d,\Delta_1,\ell_1}$	$\mathbf{G}_{d,\Delta_2,\ell_2}$	$\mathbf{G}_{d,\Delta_5,\ell_5}$	$\mathbf{G}_{d,\Delta_7,\ell_7}$
facet-9	$\mathbf{G}_{d,\Delta_1,\ell_1}$	$\mathbf{G}_{d,\Delta_2,\ell_2}$	$\mathbf{G}_{d,\Delta_7,\ell_7}$	$\mathbf{G}_{d,\Delta_8,\ell_8}$
facet-10	$\mathbf{G}_{d,\Delta_1,\ell_1}$	$\mathbf{G}_{d,\Delta_2,\ell_2}$	$\mathbf{G}_{d,\Delta_8,\ell_8}$	$\mathbf{G}_{d,\Delta_9,\ell_9}$
facet-11	$\mathbf{G}_{d,\Delta_2,\ell_2}$	$\mathbf{G}_{d,\Delta_4,\ell_4}$	$\mathbf{G}_{d,\Delta_5,\ell_5}$	$\mathbf{G}_{d,\Delta_7,\ell_7}$
facet-12	$\mathbf{G}_{d,\Delta_2,\ell_2}$	$\mathbf{G}_{d,\Delta_4,\ell_4}$	$\mathbf{G}_{d,\Delta_7,\ell_7}$	$\mathbf{G}_{d,\Delta_8,\ell_8}$
facet-13	$\mathbf{G}_{d,\Delta_2,\ell_2}$	$\mathbf{G}_{d,\Delta_4,\ell_4}$	$\mathbf{G}_{d,\Delta_8,\ell_8}$	$\mathbf{G}_{d,\Delta_9,\ell_9}$
facet-14	$\mathbf{G}_{d,\Delta_4,\ell_4}$	$\mathbf{G}_{d,\Delta_5,\ell_5}$	$\mathbf{G}_{d,\Delta_7,\ell_7}$	$\mathbf{G}_{d,\Delta_8,\ell_8}$
facet-15	$\mathbf{G}_{d,\Delta_4,\ell_4}$	$\mathbf{G}_{d,\Delta_5,\ell_5}$	$\mathbf{G}_{d,\Delta_8,\ell_8}$	$\mathbf{G}_{d,\Delta_9,\ell_9}$
facet-16	$\mathbf{G}_{d,\Delta_5,\ell_5}$	$\mathbf{G}_{d,\Delta_6,\ell_6}$	$\mathbf{G}_{d,\Delta_7,\ell_7}$	$\mathbf{G}_{d,\Delta_9,\ell_9}$
facet-17	$\mathbf{G}_{d,\Delta_5,\ell_5}$	$\mathbf{G}_{d,\Delta_7,\ell_7}$	$\mathbf{G}_{d,\Delta_8,\ell_8}$	$\mathbf{G}_{d,\Delta_9,\ell_9}$

Table 6: Various facets for $D = 2N = 4$ for 2d ising model, where $\mathbf{G}_{d,\Delta_i,\ell_i}$ are the block vectors for $D = 2N = 4$ and $\mathbf{G}_{d,\Delta_0,\ell_0} = (1, 0, 0, 0, 0)$

appendix we investigate one such case namely ordering in terms of increasing value of $\Delta - \ell$, see table (7). For the 2d Ising model, there are degenerate values of $\Delta - \ell$. From the spectrum eq (B.1) (we consider the first 9 operators) there are $3! \times 3! \times 3! = 216$ degeneracy. Out of all 216 orderings there are only 4 combinations that give positive determinants and these ordering are

$$\begin{aligned}
1) \quad & \Delta_1 = 2, \Delta_2 = 4, \Delta_3 = 6, \Delta_4 = 7, \Delta_5 = 1, \Delta_6 = 5., \Delta_7 = 8, \Delta_8 = 6., \Delta_9 = 4. \\
& \ell_1 = 2, \ell_2 = 4, \ell_3 = 6, \ell_4 = 6, \ell_5 = 0, \ell_6 = 4, \ell_7 = 4, \ell_8 = 2, \ell_9 = 0 \\
2) \quad & \Delta_1 = 2, \Delta_2 = 4, \Delta_3 = 6, \Delta_4 = 7, \Delta_5 = 1, \Delta_6 = 5, \Delta_7 = 6., \Delta_8 = 4., \Delta_9 = 8. \\
& \ell_1 = 2, \ell_2 = 4, \ell_3 = 6, \ell_4 = 6, \ell_5 = 0, \ell_6 = 4, \ell_7 = 2, \ell_8 = 0, \ell_9 = 4 \\
3) \quad & \Delta_1 = 4, \Delta_2 = 6, \Delta_3 = 2, \Delta_4 = 7, \Delta_5 = 1, \Delta_6 = 5., \Delta_7 = 8, \Delta_8 = 6, \Delta_9 = 4. \\
& \ell_1 = 4, \ell_2 = 6, \ell_3 = 2, \ell_4 = 6, \ell_5 = 0, \ell_6 = 4, \ell_7 = 4, \ell_8 = 2, \ell_9 = 0 \\
4) \quad & \Delta_1 = 4, \Delta_2 = 6., \Delta_3 = 2, \Delta_4 = 7, \Delta_5 = 1, \Delta_6 = 5., \Delta_7 = 6, \Delta_8 = 4., \Delta_9 = 8. \\
& \ell_1 = 4, \ell_2 = 6, \ell_3 = 2, \ell_4 = 6, \ell_5 = 0, \ell_6 = 4, \ell_7 = 2, \ell_8 = 0, \ell_9 = 4
\end{aligned} \tag{B.3}$$

Even though these ordering give positive determinants but we did not find any general pattern of the ordering. Also in the table, we have ordered degenerate operators with respect to increasing Δ . Other possible orderings do not change the conclusion. It may be possible that some complicated combination of Δ and ℓ can lead to cyclic polytope structure in even small Δ range which we have not found so far.

i	$\langle \vec{G}_{d,\Delta_1,\ell_1}, \vec{G}_{d,\Delta_2,\ell_2}, \dots, \vec{G}_{d,\Delta_i,\ell_i} \rangle$	i	$\langle \vec{G}_{d,\Delta_1,\ell_1}, \vec{G}_{d,\Delta_2,\ell_2}, \dots, \vec{G}_{d,\Delta_i,\ell_i} \rangle$
1	5.72525	1	5.72525
2	183.694	2	183.694
3	33303.3	3	33303.3
4	-1.32982×10^6	4	9.91382×10^6
5	1.08811×10^8	5	1.37549×10^9
6	1.28685×10^{11}	6	1.28685×10^{11}
7	6.96021×10^{10}	7	2.97071×10^{14}
8	-8.39807×10^{10}	8	1.36497×10^{15}
9	-1.80068×10^{12}	9	1.80068×10^{12}

Table 7: Left: Determinants of first few operators of 2D Ising model using equation (2.1), spectrum (B.1) in increasing order of $\Delta - \ell$, here we have ordered the degenerate ordering in increasing ordering of Δ and Right: determinants of first few operators of 2D Ising model using 2.1, spectrum (B.1) in increasing order of $\Delta - \ell$ using spectrum (1) of eq (B.3).

Remarks

The numbers listed in table 5 are found using (2.1). Some determinants are negative which show that $P(c_\ell)$ is not a cyclic polytope. However, we get positive numbers if we use (2.6). Also if one calculates for each ℓ separately then all the determinants are positive. This means that each spin- ℓ vectors lead to cyclic polytopes while the weighted Minkowski sum is not. However, as we have shown earlier, the approximate block in eq.(2.6) is in very good agreement numerically with the exact block (2.1). Therefore, in some approximate sense $P(c_\ell)$ is also a cyclic polytope.

Also we have explicitly calculated the faces of the polytopes e.g. table (6) and we find that $P(c_\ell)$ is not a cyclic polytopes and for each ℓ separately they from cyclic polytopes. And we find that $P(c_\ell)$ is cyclic polytopes if we use (2.6).

C Analytic kink analysis

Here will briefly elaborate on our attempts to track down the location of the kink, in the cyclic polytope picture in section 7, analytically. By plugging in the asymptotic blocks to the $1/\Delta_S$ order which can be easily found using eq. (2.3), one can easily find that the the largest zero of det_3 (obtained by expanding the determinant to $O(\Delta_S^2)$) which we will denote by $\zeta_0^{(3)}$ is given by

$$\zeta_0^{(3)} = 3\sqrt{2}\Delta_\phi + 3 - \frac{3}{\sqrt{2}}. \quad (\text{C.1})$$

On the other hand, the location of the largest zero of det_4 is given by a 5-th order polynomial equation (obtained by expanding the determinant to $O(\Delta_S^2)$) whose roots cannot be found analytically. However, we are interested in crossing of the zeros of det_3 and det_4 so we will just put the largest zero of det_4 as

$$\zeta_0^{(4)} = \zeta_0^{(3)} + \delta, \quad (\text{C.2})$$

and Taylor expand in δ to obtain a simpler equation. This equation now (in the context of the analysis in section 7) depends on the Δ_8 . We can expand in the limit where $\Delta_8 \gg 1$ and find an approximate equation whose (positive) root gives us the value of Δ_ϕ at the kink. This works out to be

$$\Delta_\phi = \frac{-33 - 24\sqrt{2} + \sqrt{4277 + 3024\sqrt{2}}}{16(17 + 12\sqrt{2})} \approx 0.0469974, \quad (\text{C.3})$$

using which we find

$$\Delta_S \approx 1.07808. \quad (\text{C.4})$$

Considering the fact that we have used only the $1/\Delta_S$ approximation of the block and we are trying to track down a kink at $\Delta_S \sim O(1)$, it is not surprising that we do not get a very precise location which is closer to $(\Delta_\phi, \Delta_S) = (0.08, 1.2)$ but nonetheless this would be a good starting point to see if a systematic solution can be worked out by retaining higher order $1/\Delta_S$ terms.

D Adding spin and kink

In this appendix we consider the effect of adding spin to the analysis of bounds on the leading scalar dimension Δ_S . In the diagonal limit, it seems that position of spin does not move much, even if we add spins. See figure (11). We will study this effect in detail in an upcoming work [21].

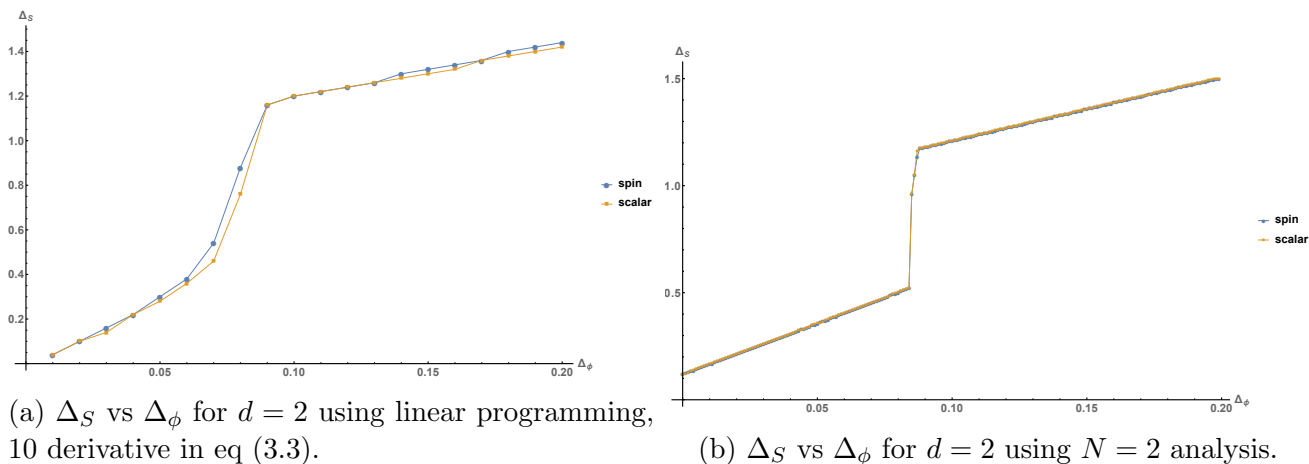


Figure 11: Bound for the leading scalar dimension including spins in the spectrum. In each plot, the blue line is obtained considering up to spin $\ell = 6$ in the analysis. Yellow line is only considering the scalar in the spectrum

E Issues with scalars

It is possible that for small Δ is it possible to get the determinants $\langle \vec{G}_{d,\Delta_1,\ell_1}, \vec{G}_{d,\Delta_2,\ell_2}, \dots, \vec{G}_{d,\Delta_D,\ell_D} \rangle < 0$. For the 2d and 3d Ising models, this does not happen for each spin separately. We rigorously checked

the determinants scanning various Δ in Mathematica. For example, for only scalars ¹³ if we assume spectrum like $\Delta_j = \frac{d-2}{2} + a \times j$ then to have positivity the minimum ¹⁴ value of a is

$$\begin{aligned} a &> 0.0326, \quad d = 2 \\ a &> 0.1906, \quad d = 3 \\ a &> 0.2395, \quad d = 4, \end{aligned} \tag{E.1}$$

for $D = 2N + 1 = 7$ dimensional polytope.

Note that from definition of F_{mn} eq (3.16)

$$\frac{\partial^m G_{d,\Delta_j,\ell}(z)|_{z=1/2}}{m!} = \sum_n (\Delta_j - \Delta)^n \frac{F_{m,n}}{n!} \tag{E.2}$$

We want to analyse the behaviour of $\langle \vec{G}_{d,\Delta_1,\ell}, \vec{G}_{d,\Delta_2,\ell}, \dots, \vec{G}_{d,\Delta_D,\ell} \rangle$ assuming the spectrum for fixed spin ℓ , $\Delta_j = \Delta + \delta_j$, where δ_j is small and $\delta_{j+1} > \delta_j$ *i.e* this spectrum respects the increasing ordering in Δ_j

$$\langle \vec{G}_{d,\Delta_1,\ell}, \vec{G}_{d,\Delta_2,\ell}, \dots, \vec{G}_{d,\Delta_D,\ell} \rangle = \alpha_D(d, \Delta, \ell) \prod_{i < j} (\delta_j - \delta_i) + \mathcal{O}\left(\delta^{\frac{D(D-1)}{2}+1}\right) ; D > 2 \tag{E.3}$$

where

$$\alpha_D(d, \Delta, \ell) = \det \begin{pmatrix} F_{0,0} & F_{1,0} & \dots & \dots & F_{2N+1,0} \\ F_{0,1} & F_{1,1} & \dots & \dots & \dots \\ \dots & \dots & \frac{F_{i,j}}{j!} & \dots & \dots \\ \dots & \dots & \dots & \dots & \dots \\ \frac{F_{0,D}}{D!} & \dots & \dots & \dots & \frac{F_{D,D}}{D!} \end{pmatrix}. \tag{E.4}$$

So we conclude that if $\alpha_D(d, \Delta, \ell)$'s are positive whatever small number δ_j is as long as they are ordered (*i.e* $\delta_{j+1} > \delta_j$) the cyclicity holds. Also note that α_D defined in [14, eq (5.15)] is equal to our $\alpha_D(d, \Delta, \ell)$

$$\alpha_D(d = 1, \Delta = 0, \ell = 0) = \alpha_D \tag{E.5}$$

We find

$$|\mathbf{K}_D(d, \Delta, \ell)| = \left(\prod_{j=0}^D j! \right) \alpha_D(d, \Delta, \ell). \tag{E.6}$$

Knowing $g_1 > 0, g_2 > 0$ it is then recursively true that for positivity of D dimensional polytope it is sufficient that $g_i > 0, \forall i, 1 \leq i \leq D$.

¹³Only scalars create problems near the unitary value of Δ as is clear from figure (4, 5)

¹⁴One can fine grain it by increasing precision in Mathematica which we have not done here.

Note

This analysis shows how $\mathbf{K}_i(d, \Delta, \ell)$ appears. We have checked analytically that our definition of g_i 's in terms of $\mathbf{K}_i(d, \Delta, \ell)$ eq (3.18) is same given in [14]. Even though we don't have first hand proof of it. We guess the formula by observing first three g_i 's and verified it till g_8 that it is true.

Also it is important to mention that Mathematica has some numerical issues evaluating the determinants eq (3.15). It gives very small negative numbers ($\sim 10^{-50}$) or very big negative numbers ($\sim 10^{50}$) when the spacing δ_j is very small even if in the region of Δ for which g_i 's are positive. That this should not happen is clear from the above analysis.

References

- [1] R. Rattazzi, V. S. Rychkov, E. Tonni and A. Vichi, "Bounding scalar operator dimensions in 4D CFT," *JHEP* **0812**, 031 (2008) [arXiv:0807.0004 [hep-th]].
- [2] S. Rychkov and P. Yvernay, "Remarks on the Convergence Properties of the Conformal Block Expansion," *Phys. Lett. B* **753**, 682 (2016) [arXiv:1510.08486 [hep-th]].
- [3] S. El-Showk, M. F. Paulos, D. Poland, S. Rychkov, D. Simmons-Duffin and A. Vichi, "Solving the 3D Ising Model with the Conformal Bootstrap," *Phys. Rev. D* **86**, 025022 (2012) [arXiv:1203.6064 [hep-th]].
S. El-Showk, M. F. Paulos, D. Poland, S. Rychkov, D. Simmons-Duffin and A. Vichi, "Solving the 3d Ising Model with the Conformal Bootstrap II. c-Minimization and Precise Critical Exponents," *J. Stat. Phys.* **157**, 869 (2014) [arXiv:1403.4545 [hep-th]].
F. Kos, D. Poland, D. Simmons-Duffin and A. Vichi, "Precision islands in the Ising and O(N) models," *JHEP* **1608**, 036 (2016) [arXiv:1603.04436 [hep-th]].
- [4] D. Poland, S. Rychkov and A. Vichi, "The Conformal Bootstrap: Theory, Numerical Techniques, and Applications," [arXiv:1805.04405 [hep-th]].
- [5] V. S. Rychkov and A. Vichi, "Universal Constraints on Conformal Operator Dimensions," *Phys. Rev. D* **80**, 045006 (2009) [arXiv:0905.2211 [hep-th]].
- [6] A. M. Polyakov, "Nonhamiltonian approach to conformal quantum field theory," *Zh. Eksp. Teor. Fiz.* **66**, 23 (1974).
- [7] K. Sen and A. Sinha, "On critical exponents without Feynman diagrams," *J. Phys. A* **49**, no. 44, 445401 (2016) [arXiv:1510.07770 [hep-th]].
- [8] R. Gopakumar, A. Kaviraj, K. Sen and A. Sinha, "Conformal Bootstrap in Mellin Space," *Phys. Rev. Lett.* **118**, no. 8, 081601 (2017) [arXiv:1609.00572 [hep-th]].
- [9] R. Gopakumar, A. Kaviraj, K. Sen and A. Sinha, "A Mellin space approach to the conformal bootstrap," *JHEP* **1705**, 027 (2017) [arXiv:1611.08407 [hep-th]].
- [10] P. Dey, A. Kaviraj and A. Sinha, "Mellin space bootstrap for global symmetry," *JHEP* **1707**, 019 (2017) [arXiv:1612.05032 [hep-th]].

- [11] P. Dey, K. Ghosh and A. Sinha, “Simplifying large spin bootstrap in Mellin space,” JHEP **1801**, 152 (2018) [arXiv:1709.06110 [hep-th]].
- [12] R. Gopakumar and A. Sinha, “On the Polyakov-Mellin bootstrap,” JHEP **1812**, 040 (2018) [arXiv:1809.10975 [hep-th]].
- [13] D. Mazac and M. F. Paulos, “The Analytic Functional Bootstrap I: 1D CFTs and 2D S-Matrices,” arXiv:1803.10233 [hep-th].
D. Mazac and M. F. Paulos, “The Analytic Functional Bootstrap II: Natural Bases for the Crossing Equation,” arXiv:1811.10646 [hep-th].
A. Kaviraj and M. F. Paulos, “The Functional Bootstrap for Boundary CFT,” [arXiv:1812.04034[hep-th]].
- [14] N. Arkani-Hamed, Y. T. Huang and S. H. Shao, “On the Positive Geometry of Conformal Field Theory,” arXiv:1812.07739 [hep-th].
- [15] M. Hogervorst, H. Osborn and S. Rychkov, “Diagonal Limit for Conformal Blocks in d Dimensions,” JHEP **1308**, 014 (2013) [arXiv:1305.1321 [hep-th]].
- [16] B. Mukhametzhanov and A. Zhiboedov, “Analytic Euclidean Bootstrap,” arXiv:1808.03212 [hep-th].
- [17] Christophe Weibel, “Minkowski sum of polytopes: Combinatorics and computation,” PhD Thesis, 2007.
- [18] Yudell L. Luke, “The Special Functions and Their Approximations, Vol-1” ACADEMIC PRESS, 1969.
- [19] S. Caron-Huot, “Analyticity in Spin in Conformal Theories,” JHEP **1709**, 078 (2017) [arXiv:1703.00278[hep-th]].
- [20] D. Simmons-Duffin, “The Lightcone Bootstrap and the Spectrum of the 3d Ising CFT,” JHEP **1703**, 086 (2017) [arXiv:1612.08471 [hep-th]].
- [21] Y. Huang, A. Sinha, Li Wei, A. Zahed, in preparation.